ELSEVIER

Journal of Geometry and Physics 46 (2003) 308–354

JOURNAL OF GEOMETRY AND PHYSICS

www.elsevier.com/locate/jgp

Generalized lattice gauge theory, spin foams and state sum invariants

Robert Oeckl

Centre de Physique Théorique, CNRS Luminy, Case 907, F-13288 Marseille Cedex 9, France

Received 2 May 2002

Abstract

We construct a generalization of pure lattice gauge theory (LGT) where the role of the gauge group is played by a tensor category. The type of tensor category admissible (spherical, ribbon, symmetric) depends on the dimension of the underlying manifold (≤ 3, ≤ 4, any). Ordinary LGT is recovered if the category is the (symmetric) category of representations of a compact Lie group. In the weak coupling limit we recover discretized BF-theory in terms of a coordinate-free version of the spin foam formulation. We work on general cellular decompositions of the underlying manifold.

In particular, we are able to formulate LGT as well as spin foam models of BF-type with quantum gauge group (in dimension ≤ 4) and with supersymmetric gauge group (in any dimension).

Technically, we express the partition function as a sum over diagrams denoting morphisms in the underlying category. On the LGT side this enables us to introduce a generalized notion of gauge fixing corresponding to a topological move between cellular decompositions of the underlying manifold. On the BF-theory side this allows a rather geometric understanding of the state sum invariants of Turaev/Viro, Barrett/Westbury and Crane/Yetter which we recover.

The construction is extended to include Wilson loop and spin network type observables as well as manifolds with boundaries. In the topological (weak coupling) case this leads to topological quantum field theories with or without embedded spin networks.

MSC: 57M27; 81T25; 81T13; 57R56; 81R50

Subj. Class.: Quantum field theory

Keywords: Lattice gauge theory; State sum invariants; Quantum groups; Spin foams

1. Introduction

We start by describing the main motivations of the present work.

E-mail address: r.oeckl@cpt.univ-mrs.fr (R. Oeckl).

0393-0440/02/$ – see front matter © 2002 Elsevier Science B.V. All rights reserved.
PII: S0393-0440(02)00148-1

Lattice gauge theory (LGT) is our most successful approach to date at describing the non-perturbative regime of the standard model, such as bound states of QCD. If the gauge group is Abelian there is a well known duality transformation exchanging the strong with the weak coupling regime [1]. At the same time group valued degrees of freedom are replaced with character valued degrees of freedom. As the latter also form a group the dual theory is again a gauge theory living on the dual lattice. Even in the non-Abelian case a "dual" formulation is possible where the degrees of freedom are "representation valued". While this is not a gauge theory anymore it is known to be expressible as a (modified) spin foam model [2]. This dual model was explicitly constructed for hypercubic lattices in [3]. There, it was also shown to be strong–weak dual to the ordinary formulation of LGT. Thus, a better understanding of this formulation and improved techniques to handle it appear of great value in order to extract a strong-coupling expansion.

Quantum groups have their origin as symmetries of integrable models. Thus, it is natural to ask whether they can be "gauged", i.e., whether one could formulate gauge theories with quantum groups. Indeed, this is supported, e.g., by an analysis of Chern–Simons theory where a necessary regularization of the path integral naturally leads to quantum gauge groups [4]. At the non-perturbative level LGT appears clearly the most suitable starting point for such a development. Indeed, a proposal for a q-deformed LGT in three dimensions has been made [5]. In four dimensions a generalized LGT for ribbon categories was constructed on simplicial decompositions of the underlying manifold [6]. A unified approach, preferably for general cellular decompositions, is clearly desirable.

Spin foams have emerged as a description of space–time both in the canonical loop approach to quantum gravity as well as in covariant path integral approaches [7]. On the other hand, pure quantum gravity in three dimensions turns out to be essentially quantum BF-theory, which is topological [8]. Indeed, a well defined path integral description of BF-theory can be given in the spin foam framework. A predecessor to these ideas is the state sum model of Ponzano and Regge [9]. q-deformations of the gauge group come about when a cosmological constant is included [10]. Spin foam models of BF-theory have recently been the starting point for several proposals for quantum gravity also in four dimensions [11] (see also the review [12]).

A completely new type of algebraic topology started to emerge in the 1980s, initiated by the application of quantum field theoretic ideas to low-dimensional topology. In particular, this led to new kinds of topological invariants of manifolds and the notion of topological quantum field theory (TQFT). The most prominent invariants are the surgery invariant of Reshetikhin and Turaev in three dimensions [13], the state sum invariant of Turaev and Viro in three dimensions [14,15] and the state sum invariant of Crane and Yetter in four dimensions [16,17]. All those invariants require a (quantum) group or, more generally, a certain type of category as input. It turns out that using ordinary groups (as compared to quantum groups) does not lead to interesting new invariants. The reason for this can be seen to lie in the fact that the quantum groups "feel" more about the topology than the ordinary groups. However, this remains somewhat obscure in the standard approaches to the invariants.

This work aims to contribute to the above-mentioned developments as well as to improve our understanding of the connections between them.

We construct a generalization of pure LGT where the role of the gauge group is played by a monoidal (or tensor) category. Ordinary LGT is recovered if the category is taken to be

the category of representations of a compact Lie group. We make heavy use of the relation between (types of) tangle diagrams and (types of) monoidal categories as developed in [18–20]. We suitably extend this to a diagrammatic calculus which allows to express the partition function of LGT in a purely diagrammatic way. More concretely, the diagram defining the partition function as a morphism in the given category is constructed from a cellular decomposition of the underlying manifold. This diagram can be considered as the "projection" onto the plane of a graph embedded into the manifold.

The cases of symmetric and nonsymmetric categories are different in an essential way. In the former case a lattice (combinatorial 2-complex) is sufficient to define LGT. In particular, this lattice can be obtained as the dual 2-skeleton of a cellular decomposition of a manifold of arbitrary dimension which need not be orientable. In the nonsymmetric case an orientable manifold is required and the orientation indeed enters into the construction of LGT. Furthermore, the dimension of the manifold is restricted by the type of category. Concretely, the maximal allowed dimension is 2, 3 and 4 for pivotal, spherical and ribbon categories, respectively. Indeed, the geometric nature of our construction makes this connection between the dimension and the admissible type of category rather transparent through the isotopy properties characterizing the tangle diagrams associated with the category.

The gauge invariance properties of conventional LGT are shown to extend to our generalized LGT. Gauge fixing can be reexpressed as the invariance of the partition function under a certain topological move relating different cellular decompositions of the manifold. The standard Wilson loop and spin network observables are included in our generalized LGT. However, in the nonsymmetric case the maximal allowed dimension for a given type of category drops by 1. Extending our formulation to manifolds with boundaries we obtain (as expected) spin networks as states on the boundary and consider briefly the construction of the associated TQFTs.

In the weak coupling limit we obtain (discretized) BF-theory and recover the above-mentioned state sum invariants of Turaev and Viro [14], Barrett and Westbury [15] and Crane and Yetter [16,17].

Section 2 introduces the relevant types of categories, their diagrammatics and the notion of semisimplicity. Section 3 reviews how those categories arise as categories of representations of groups, supergroups and quantum groups. Furthermore, the diagrammatic calculus as well as the notion of semisimplicity is further developed for these cases. The partition function of generalized LGT is introduced in Section 4.1. First, a diagrammatic representation of the partition function of ordinary LGT is derived. Then, the generalization to different types of categories is performed. Gauge symmetry and gauge fixing are considered in Section 5. Observables of Wilson loop and spin network type are implemented in Section 6. The partition function is extended to manifolds with boundaries in Section 7. (Generalized) spin networks emerge as boundary states and the construction of the relevant TQFTs in the topological case is sketched. Special cases are considered in Section 8. In particular, we consider how the spin foam picture emerges. We discuss the topological weak coupling limit (BF-theory) and the specialization to the various state sum invariants. An outlook is presented in Section 9.

Propositions and lemmas for which the proof is not included are either to be found in the given references or verified straightforwardly.

2. Categories and diagrams

In this section we introduce the various types of categories which are to play the role of the "gauge symmetry" for generalized LGT. Furthermore, we introduce the associated diagrammatics which is instrumental in our formulation of LGT.

2.1. Monoidal categories with structure

We start by introducing the necessary categorial notions. A standard reference for general category theory and monoidal categories is [21]. Pivotal, spherical and ribbon categories as well as their diagrammatic representations are introduced in [18], [20] and [19], respectively.

In the following, category is always taken to mean $\mathbb{C}$-linear category. By this we mean that the set $\mathrm{Mor}(V, W)$ of morphisms from an object V to an object W forms a vector space over the field $\mathbb{C}$. Furthermore, the composition of morphisms

$$\mathrm{Mor}(U, V) \times \mathrm{Mor}(V, W) \to \mathrm{Mor}(U, W), \qquad (f, g) \mapsto g \circ f$$

is required to be bilinear.

Definition 2.1. A (strict) *monoidal category* is a category $\mathcal{C}$ together with a bifunctor $\otimes : \mathcal{C} \times \mathcal{C} \to \mathcal{C}$ (called *tensor product*) and a choice of unit element $\mathbf{1} \in \mathcal{C}$. Furthermore we require the equalities $(U \otimes V) \otimes W = U \otimes (V \otimes W)$ and $U \otimes \mathbf{1} = U = \mathbf{1} \otimes U$. We also require that $\mathrm{Mor}(\mathbf{1}, \mathbf{1}) = \mathbb{C}$ and the monoidal structure on morphisms be identified with their tensor product as vectors.

Definition 2.2. A *rigid monoidal category* is a monoidal category $\mathcal{C}$ together with a contravariant functor $* : \mathcal{C} \to \mathcal{C}$ called *dual* and morphisms $\mathrm{ev}_V : V^* \otimes V \to \mathbf{1}$ (*evaluation*), $\mathrm{coev}_V : \mathbf{1} \to V \otimes V^*$ (*coevaluation*) such that

$$(\mathrm{id}_V \otimes \mathrm{ev}_V) \circ (\mathrm{coev}_V \otimes \mathrm{id}_V) = \mathrm{id}_V, \qquad (\mathrm{ev}_V \otimes \mathrm{id}_{V^*}) \circ (\mathrm{id}_{V^*} \otimes \mathrm{coev}_V) = \mathrm{id}_{V^*}$$

and for a morphism $\Phi : V \to W$ we have its dual $\Phi^* : W^* \to V^*$ given by

$$\Phi^* = (\mathrm{ev}_W \otimes \mathrm{id}_{V^*}) \circ (\mathrm{id}_{W^*} \otimes \Phi \otimes \mathrm{id}_{V^*}) \circ (\mathrm{id}_{W^*} \otimes \mathrm{coev}_V).$$

Definition 2.3. Let $\mathcal{C}$ be a rigid monoidal category together with a natural equivalence $\tau_V : V \mapsto V^{**}$ such that $\tau_V \otimes \tau_W = \tau_{V \otimes W}$ and $\tau_{V^*}^{-1} = (\tau_V)^*$. Define $\widetilde{\mathrm{ev}}_V : V \otimes V^* \to \mathbf{1}$ and $\widetilde{\mathrm{coev}}_V : \mathbf{1} \to V^* \otimes V$ as

$$\widetilde{\mathrm{ev}}_V := \mathrm{ev}_{V^*} \circ (\tau_V \otimes \mathrm{id}_{V^*}), \qquad \widetilde{\mathrm{coev}}_V := (\mathrm{id}_{V^*} \otimes \tau_V^{-1}) \circ \mathrm{coev}_{V^*}.$$

If for all morphisms $\Phi : V \to W$ the equality

$$\Phi^* = (\mathrm{id}_{V^*} \otimes \widetilde{\mathrm{ev}}_W) \circ (\mathrm{id}_{V^*} \otimes \Phi \otimes \mathrm{id}_{W^*}) \circ (\widetilde{\mathrm{coev}}_V \otimes \mathrm{id}_{W^*})$$

holds we call $\mathcal{C}$ a *pivotal category*. For a morphism $\Phi : V \to V$ define $\mathrm{tr}_-(\Phi) : \mathbf{1} \to \mathbf{1}$ and $\mathrm{tr}_+(\Phi) : \mathbf{1} \to \mathbf{1}$ as

$$\mathrm{tr}_-(\Phi) := \mathrm{ev}_V \circ (\mathrm{id}_{V^*} \otimes \Phi) \circ \widetilde{\mathrm{coev}}_V, \qquad \mathrm{tr}_+(\Phi) := \widetilde{\mathrm{ev}}_V \circ (\Phi \otimes \mathrm{id}_{V^*}) \circ \mathrm{coev}_V.$$

For an object V define morphisms $\mathbf{1} \to \mathbf{1}$ as

$$\mathrm{loop}_- V := \mathrm{tr}_-(\mathrm{id}_V), \qquad \mathrm{loop}_+ V := \mathrm{tr}_+(\mathrm{id}_V).$$

Lemma 2.4. *In a pivotal category the identities* $\mathrm{tr}_-(\Phi) = \mathrm{tr}_+(\Phi^*)$ *and* $\mathrm{tr}_+(\Phi) = \mathrm{tr}_-(\Phi^*)$ *hold for any morphism* Φ.

Definition 2.5. A *spherical category* is a pivotal category such that for all objects V and morphisms $\Phi : V \to V$ the equality $\mathrm{tr}_-(\Phi) = \mathrm{tr}_+(\Phi)$ holds. Write $\mathrm{tr} := \mathrm{tr}_+ = \mathrm{tr}_-$ and $\mathrm{loop} := \mathrm{loop}_+ = \mathrm{loop}_-$.

Definition 2.6. A *braided monoidal category* is a monoidal category together with a natural equivalence $\psi_{V,W} : V \otimes W \to W \otimes V$ (called *braiding*) such that the following conditions hold:

$$\psi_{U\otimes V,W} = (\psi_{U,W} \otimes \mathrm{id}_V) \circ (\mathrm{id}_U \otimes \psi_{V,W}),$$
$$\psi_{U,V\otimes W} = (\mathrm{id}_V \otimes \psi_{U,W}) \circ (\psi_{U,V} \otimes \mathrm{id}_W), \qquad \psi_{V,\mathbf{1}} = \mathrm{id}_V = \psi_{\mathbf{1},V}.$$

Definition 2.7. A *ribbon category* is a rigid braided monoidal category together with a natural equivalence $\nu_V : V \to V$ such that

$$\nu_{V\otimes W} = \psi^{-1}_{V,W} \circ \psi^{-1}_{W,V}(\nu_V \otimes \nu_W), \qquad \nu_{\mathbf{1}} = \mathrm{id}_{\mathbf{1}}, \qquad \nu_{V^*} = (\nu_V)^*.$$

Lemma 2.8. *A ribbon category is a spherical category by setting*

$$\tau_V := (\mathrm{ev}_V \otimes \mathrm{id}_{V^{**}}) \circ (\psi^{-1}_{V^*,V} \otimes \mathrm{id}_{V^{**}}) \circ (\nu_V \otimes \mathrm{coev}_{V^*}).$$

Definition 2.9. A *symmetric category* is a rigid monoidal category together with a natural equivalence $\psi_{V,W} : V \otimes W \to W \otimes V$ such that the following conditions hold:

$$\psi_{U\otimes V,W} = (\psi_{U,W} \otimes \mathrm{id}_V) \circ (\mathrm{id}_U \otimes \psi_{V,W}),$$
$$\psi_{U,V\otimes W} = (\mathrm{id}_V \otimes \psi_{U,W}) \circ (\psi_{U,V} \otimes \mathrm{id}_W),$$
$$\psi_{W,V} \circ \psi_{V,W} = \mathrm{id}_{V\otimes W}, \qquad \psi_{V,\mathbf{1}} = \mathrm{id}_V = \psi_{\mathbf{1},V}.$$

Note that the usual definition of "symmetric" does not imply rigidity. We include it here for uniformity of terminology.

Lemma 2.10. *A symmetric category is a ribbon category by noting that the symmetric structure* ψ *is a self-inverse braiding and by setting* $\nu_V := \mathrm{id}_V$.

2.2. Diagrams and isotopy invariance

The types of categories we will be mainly interested in are the *pivotal*, *spherical*, *ribbon*, and *symmetric* categories. Morphisms in those categories can be conveniently described by directed tangle diagrams with additional structure. Remarkably, the denoted morphisms

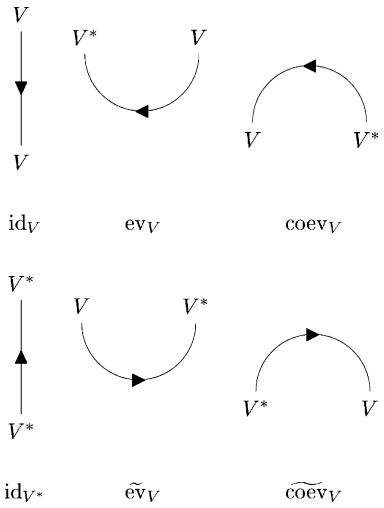

Fig. 2.1. Elementary tangle diagrams and their assigned morphisms.

remain invariant under certain isotopies of these diagrams. This plays a key role in the construction of the partition function of generalized LGT. We introduce this diagrammatics in this section.

We start by considering the pivotal case. A diagram (without coupons) consists of a finite number of non-intersecting lines in the plane. The lines end at the top or bottom line of the diagram or form closed loops. Each line carries an object label and an arrow. A diagram as a whole defines a morphism in the category. If the object labels of the lines ending at the top are $V_1, \ldots, V_n$ and the ones ending at the bottom are $W_1, \ldots, W_m$ it defines a morphism $V_1 \otimes \cdots \otimes V_n \to W_1 \otimes \cdots \otimes W_m$. For lines with an arrow pointing upwards the respective object is replaced by its dual.

For elementary diagrams the assignments are listed in Fig. 2.1. Note that the unit object $\mathbf{1}$ is usually not explicitly represented in the diagrams. Diagrams placed horizontally next to each other correspond to the tensor product of morphisms. For more complicated diagrams the morphism is obtained by slicing the diagram horizontally into elementary slices and composing the corresponding morphisms from top to bottom.

We need to introduce another elementary diagram: a *coupon*. This is a rectangle which is connected to a certain number of lines on the top and the bottom (see Fig. 2.2). Furthermore, it carries a label denoting a morphism from the tensor product of the objects (or their duals) labeling the lines at the top to the corresponding tensor product at the bottom. Under the assignment of morphisms to diagrams a coupon is simply assigned the morphism with which it is labeled.

The morphism associated with such a diagram is invariant under planar isotopy. That is, any diagram that is related to a given one by an isotopy in $\mathbb{R}^2$ (holding the endpoints of lines at the top and bottom fixed) yields the same morphism. Note that a closed diagram, i.e., a diagram without endpoints denotes a morphism $\mathbf{1} \to \mathbf{1}$ and thus an element in $\mathbb{C}$.

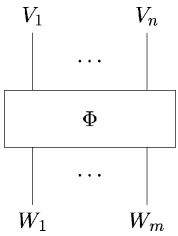

Fig. 2.2. Coupon.

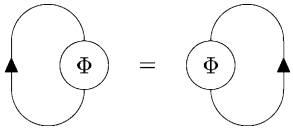

Fig. 2.3. Trace property defining a spherical category.

We now turn to the spherical case. The additional property of a spherical category as compared to a pivotal one (Definition 2.5) can be easily expressed diagrammatically (Fig. 2.3). The consequence is an enhanced isotopy invariance of the diagrammatics. That is, given a closed diagram inscribed on a 2-sphere, any isotopic deformation followed by piercing the 2-sphere at some point to identify it with the plane yields the same morphism.

For ribbon categories we need to modify the diagrammatics as follows. Instead of lines we now consider ribbons. One can think of this as equipping the lines with a *framing*. The orientation of a ribbon (i.e., the framing) at its endpoints is always "face up". In particular, a ribbon has an "upside" and a "downside" and thus an orientation. This is also true for ribbon loops, e.g., a Möbius strip is not allowed.

We also have additional elementary diagrams in the ribbon case. One must certainly be a twist of the ribbon (and its inverse). Furthermore, we allow crossings of ribbons, with a distinction between over- and under-crossings (see Fig. 2.4, where the arrows are omitted in the diagrams).

The isotopy invariance of the ribbon diagrammatics is even stronger than in the spherical case. Indeed, we can think of a diagram as obtained by projecting a ribbon tangle in $\mathbb{R}^3$ (or

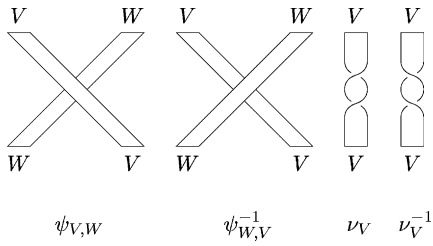

Fig. 2.4. Additional ribbon diagrams and their assigned morphisms.

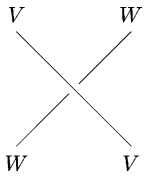

Fig. 2.5. The crossing $\psi_{V,W}$ in the symmetric case.

S^3) onto the plane. Then, the projection of any isotopic ribbon tangle in $\mathbb{R}^3$ (or S^3) will yield a diagram corresponding to the same morphism. This is because (the ribbon version of) the Reidemeister moves give rise to identities of morphisms. Note that in case of an open diagram, i.e., a diagram with endpoints, the endpoints are to be held fixed and no isotopy involving the moving of a ribbon "around" endpoints is allowed.

When drawing ribbon diagrams it is sometimes convenient and sufficient to just draw lines instead of ribbons. The convention in this case is that a line represents a ribbon which lies everywhere "face up". This is called the *blackboard framing*.

Note that as a ribbon category is in particular a spherical category, we can convert a diagram for a morphism in the latter into a diagram for the same morphism in the former. This is simply achieved by introducing the blackboard framing.

Finally we consider the case of symmetric categories. The diagrammatics is again similar to the pivotal and spherical cases. That is, we have again lines instead of ribbons. The only difference is that crossings are allowed, and there is only one type of crossing (see Fig. 2.5).

The invariance properties of the diagrammatics are the strongest in the symmetric case. Consider a set of coupons, a set of endpoints at the top and bottom and a specification of which endpoint (on the border of the diagram or on a coupon) is to be connected to which other one and with which arrow direction. This combinatorial data already specifies a morphism in the category. That is, any diagram that satisfies this combinatorial data yields the same morphism.

A symmetric category is in particular a ribbon category. Thus, we can convert the diagram for a morphism in the latter into the diagram for the same morphism in the former. This is simply achieved by removing the framing (as the twist is now trivial) and forgetting about the distinction between over- and under-crossings which become identical.

The invariance properties of the diagrammatics for the different types of categories are summarized in Table 1. By slight abuse of terminology we refer to graphs which do not live in the plane but are embedded into a manifold or lattice as diagrams in the same way

Table 1
Diagrammatic invariance for different types of categories

Type of category	Diagrammatic invariance
Pivotal	Isotopy in $\mathbb{R}^2$
Spherical	Isotopy in S^2
Ribbon	Isotopy in $\mathbb{R}^3$, S^3
Symmetric	Combinatorial

(although they do not directly define a morphism). If an explicit distinction is necessary we refer to these as *embedded diagrams* and to planar ones that are obtained from these as *projected diagrams*.

Although having historically a more restricted meaning, we define the term *spin network* here to mean precisely a diagram as considered above. Thus, there are different types of spin networks depending on the type of category. The original version is for the representation category of the group SU(2) [22]. Furthermore, there one considers only lines labeled by irreducible representations and one type of coupon (represented by a trivalent vertex), which is a suitably normalized intertwiner between three incident representations.

2.3. Semisimplicity

Recall that an object V is called simple if $\mathrm{Mor}(V, V) \cong \mathbb{C}$ as a vector space. Usually one defines a category to be semisimple if any object decomposes into a direct sum of simple objects. However, we need to adopt a more general definition which does not require direct sums [23].

Definition 2.11. A category is called *semisimple* if for each object V there exists a finite set of simple objects V_i and morphisms $f_i : V \to V_i$, $g_i : V_i \to V$ such that

$$\mathrm{id}_V = \sum_i g_i \circ f_i.$$

We call this data also a *decomposition* of V. We also require $Mor(V, W) = 0$ if V, W are simple and non-isomorphic objects.

Proposition 2.12. *Let $\mathcal{C}$ be a semisimple category. We define a morphism $T_V : V \to V$ for each object V as follows. Let V_i, $f_i : V \to V_i$, $g_i : V_i \to V$ with $i \in I$ be a decomposition of V. Let $I' := \{i \in I | V_i \cong \mathbf{1}\}$. Then*

$$T_V := \sum_{i \in I'} g_i \circ f_i.$$

This definition is well (independent of the decomposition) and gives rise to the following properties:

(a) $T_{\mathbf{1}} = \mathrm{id}_{\mathbf{1}}$.
(b) $T_V = 0$ *for V simple and* $V \ncong \mathbf{1}$.
(c) T *is a projector, i.e.,* $T_V^2 = T_V$.
(d) T *defines a natural transformation of the identity functor with itself. That is, for* $\Phi : V \to W$ *a morphism we have* $T_W \circ \Phi = \Phi \circ T_V$.

If furthermore $\mathcal{C}$ is monoidal:

(e) $T_V \otimes T_W = T_{V \otimes W} \circ (T_V \otimes \mathrm{id}_W) = T_{V \otimes W} \circ (\mathrm{id}_V \otimes T_W)$.

If $\mathcal{C}$ is rigid monoidal:

(f) T *is self-dual, i.e.,* $(T_V)^* = T_{V^*}$.

If $\mathcal{C}$ is ribbon:

(g) $\psi_{V,W} \circ (T_V \otimes \mathrm{id}_W) = \psi^{-1}_{W,V} \circ (T_V \otimes \mathrm{id}_W)$.
(h) $\nu_V \circ T_V = T_V$.

Proof. We start by showing that T is well defined. Let $\{V_i, f_i, g_i\}_{i\in I}$ and $\{\tilde{V}_j, \tilde{f}_j, \tilde{g}_j\}_{j\in J}$ be two decompositions of the object V. Define $I' := \{i \in I | V_i \cong \mathbf{1}\}$ and $J' := \{j \in J | \tilde{V}_j \cong \mathbf{1}\}$. We need to show that $T_V := \sum_{i\in I'} g_i \circ f_i$ and $\tilde{T}_V := \sum_{j\in J'} g_j \circ f_j$ are equal. Since V_i and $\tilde{V}_j$ are simple objects any morphism $\tilde{f}_j \circ g_i$ must be zero if $V_i \ncong \tilde{V}_j$. This implies

$$\begin{aligned} T_V &= \sum_{i\in I', j\in J} \tilde{g}_j \circ \tilde{f}_j \circ g_i \circ f_i = \sum_{i\in I', j\in J'} \tilde{g}_j \circ \tilde{f}_j \circ g_i \circ f_i \\ &= \sum_{i\in I, j\in J'} \tilde{g}_j \circ \tilde{f}_j \circ g_i \circ f_i = \tilde{T}_V. \end{aligned}$$

Thus, T_V is well defined. Note that the above expression also proofs the projection property (c), as the term in the middle is $\tilde{T}_V \circ T_V = T_V^2$. The properties (a) and (b) follow immediately by taking the canonical decomposition of a simple object. The proof of (d) is a small modification of the proof of well definedness. We now have two different objects V, W and a morphism $\Phi : V \to W$ sandwiched in between. Considering decompositions of V and W we get as above $\Phi \circ T_V = T_W \circ \Phi \circ T_V = T_W \circ \Phi$.

Now assume $\mathcal{C}$ to be monoidal. Let $\{V_i, f_i, g_i\}_{i\in I}$ and $\{W_j, p_j, q_j\}_{j\in J}$ be decompositions of the objects V and W and $\{U_k, a_k, b_k\}_{k\in K}$ a decomposition of $V \otimes W$. Consider the composition $b_k \circ a_k \circ (g_i \otimes q_j) \circ (f_i \otimes p_j)$. Observe that $a_k \circ (g_i \otimes q_j)$ vanishes if two of the objects V_i, W_j, U_k are isomorphic to $\mathbf{1}$ while the third one is not. Thus, defining the restricted index sets as above, summing over I', J', K or I', J, K' or I, J', K' yields the same morphism. This proves (e).

Now assume $\mathcal{C}$ to be rigid. Let $\{V_i, f_i, g_i\}_{i\in I}$ be a decomposition of the object V. Then $\{V_i^*, g_i^*, f_i^*\}_{i\in I}$ is a decomposition of V^*. As $V_i^* \cong \mathbf{1}$ iff $V_i \cong \mathbf{1}$, this implies property (f).

Now assume $\mathcal{C}$ to be ribbon. Properties (g) and (h) follow by the naturality of ψ and ν and their properties $\psi_{\mathbf{1},W} = \mathrm{id}_W = \psi^{-1}_{W,\mathbf{1}}$ and $\nu_{\mathbf{1}} = \mathrm{id}_{\mathbf{1}}$. □

Using the diagrammatic language introduced above we can represent the morphism T by a coupon. As T is defined for any object we represent it simply by a coupon without label. The properties of T can be expressed as diagrammatic identities (see Fig. 2.6).

As this will be of importance later, we note that due to "factorization" of T though the unit object $\mathbf{1}$ we can define a "braiding" composed with T also in a general monoidal category.

Definition 2.13. Let $\mathcal{C}$ be a semisimple monoidal category. Let V, W be objects in $\mathcal{C}$. Let V_i, $f_i : V \to V_i$, $g_i : V_i \to V$ with $i \in I$ be a decomposition of V, $I' := \{i \in I | V_i \cong \mathbf{1}\}$. We define $\psi_{T(V),W} : V \otimes W \to W \otimes V$ and $\psi_{W,T(V)} : W \otimes V \to V \otimes W$ as follows:

$$\psi_{T(V),W} := \sum_{i\in I'} (\mathrm{id}_W \otimes f_i) \circ (g_i \otimes \mathrm{id}_W), \quad \psi_{W,T(V)} := \sum_{i\in I'} (f_i \otimes \mathrm{id}_W) \circ (\mathrm{id}_W \otimes g_i).$$

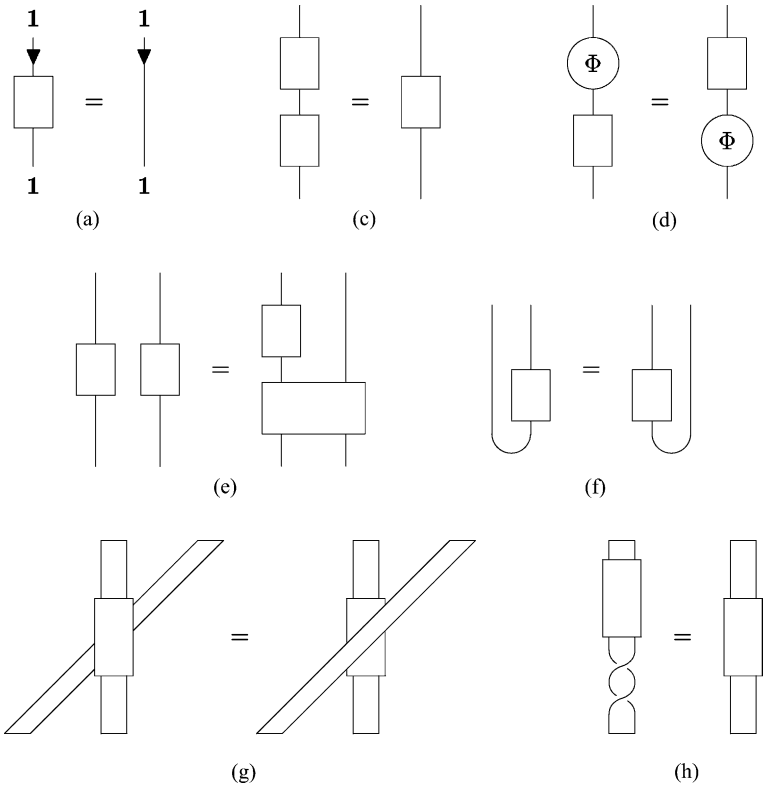

Fig. 2.6. Properties of T.

This definition simply uses the property $\mathbf{1} \otimes W = W \otimes \mathbf{1}$. Obviously, in the ribbon (or symmetric) case $\psi_{T(V),W} = \psi_{V,W} \circ (T_V \otimes \mathrm{id}_W)$ and $\psi_{W,T(V)} = \psi_{W,V} \circ (\mathrm{id}_W \otimes T_V)$. We can represent this *T-braiding* diagrammatically as in Fig. 2.7. This can be considered as an additional elementary diagram in the pivotal and spherical case. Note that its properties are analogous to those of a braiding in a symmetric category. In particular, we have the identity depicted in Fig. 2.8. (This follows by writing the T-morphism diagrammatically as a decomposition and using invariance under planar isotopy.) Indeed, this can be considered the generalization of property (h) of Proposition 2.12 to the non-ribbon case.

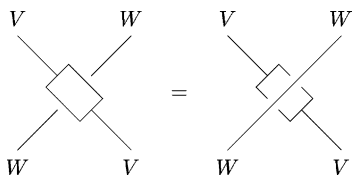

Fig. 2.7. The T-braiding $\psi_{T(V),W}$. The equality indicates that there is just one type of crossing—no distinction between “over” and “under”.

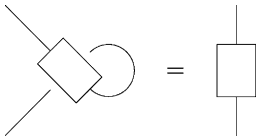

Fig. 2.8. "Twisting identity" for the T-braiding.

Important identities for the T-morphism on a tensor product are the following.

Proposition 2.14. *Let $\mathcal{C}$ be a semisimple pivotal category. For V simple we have* $\mathrm{loop}_{\pm} V \neq 0$. *For two inequivalent simple objects V and W the morphisms $T_{V^*\otimes W}$ and $T_{W\otimes V^*}$ are zero. Furthermore, for V simple we have the identities*

$$T_{V^*\otimes V} = \widetilde{\mathrm{coev}}_V \circ (\mathrm{loop}_- V)^{-1} \circ \mathrm{ev}_V, \qquad T_{V\otimes V^*} = \mathrm{coev}_V \circ (\mathrm{loop}_+ V)^{-1} \circ \widetilde{\mathrm{ev}}_V.$$

The first one is diagrammatically represented in Fig. 2.9 *while the second one is obtained by reversing all arrows.*

Proof. Let V and W be simple objects. We can use coev_V to identify the morphism spaces $\mathrm{Mor}(V^* \otimes W, \mathbf{1})$ and $\mathrm{Mor}(W, V)$. Thus, by simplicity the dimension of $\mathrm{Mor}(V^* \otimes W, \mathbf{1})$ is zero if $V \ncong W$ and 1 if $V \cong W$. This implies $T_{V^*\otimes V} = 0$ in the former case. In the latter we have $\dim(\mathrm{Mor}(V^* \otimes V, \mathbf{1})) = 1$ and in the same way $\dim(\mathrm{Mor}(\mathbf{1}, V^* \otimes V)) = 1$. This determines a one-dimensional space of morphisms $V^* \otimes V \to V^* \otimes V$ to which $T_{V^*\otimes V}$ must belong. On the other hand, $\widetilde{\mathrm{coev}}_V \circ \mathrm{ev}_V$ is an element of this space as well. Furthermore it is non-zero as it can be converted to $\mathrm{id}_{V\otimes V^*}$ by suitable composition with coev_V and $\widetilde{\mathrm{ev}}_{V^*}$. Thus, there exists a complex number λ such that $T_{V^*\otimes V} = \lambda\, \widetilde{\mathrm{coev}}_V \circ \mathrm{ev}_V$. Composing on both sides with ev_V yields $\mathrm{ev}_V = \lambda\, \mathrm{loop}_- V \mathrm{ev}_V$. As ev_V is non-zero this implies $\mathrm{loop}_- V \neq 0$ and furthermore $\lambda = (\mathrm{loop}_- V)^{-1}$.

The statements for V and V^* interchanged follow correspondingly. □

Proposition 2.15. *Let $\mathcal{C}$ be a semisimple spherical category. The permutation identity for the T-morphism on a tensor product depicted in* Fig. 2.10 *holds.* (*The object labels and arrows on the lines are arbitrary.*)

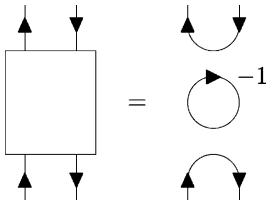

Fig. 2.9. Identity for the T-morphism on a tensor product of a simple object with its dual. All lines are labeled by the same object.

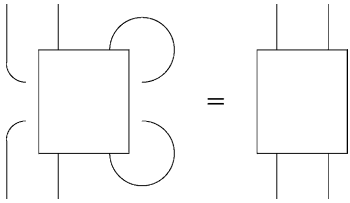

Fig. 2.10. Permutation identity for the T-morphism on a tensor product.

Proof. Choose decompositions for the two objects. Using naturality of T the identity can be reduced to an identity for the simple objects in the decomposition. Thus, we have a tensor product of two simple objects and we can apply Proposition 2.14. For the non-zero contributions we use the identity for $T_{V^*\otimes V}$ on one side of Fig. 2.10 and the one for $T_{V\otimes V^*}$ on the other. As $\mathrm{loop}_+ = \mathrm{loop}_-$ in a spherical category we obtain equality. □

3. Representation theory

In this section we review how the different types of categories arise as categories of representations of groups, supergroups and various types of Hopf algebras. We consider the issue of semisimplicity in this context. Furthermore, we develop the necessary graphical notation to represent functions on a group, supergroup or quantum group.

3.1. Groups

A relevant reference for Lie groups (representation theory, Haar measure, Peter–Weyl decomposition) is, e.g., [24]. Throughout this section, let G be a group.

3.1.1. Representation categories

In the following we consider the category of representations of G, which provides the most important example of a symmetric category. We denote the action of a group element g on a vector v by $g \triangleright v$.

Proposition 3.1. *The category $\mathcal{R}(G)$ of finite-dimensional (left) representations of a group G together with their intertwiners is a symmetric category in the following way*:

- *The monoidal structure is given by the tensor product of representations. That is, for two representation V, W we have a representation $V \otimes W$ via*

$$g \triangleright (v \otimes w) := g \triangleright v \otimes g \triangleright w.$$

  The unit object **1** *is the trivial representation.*
- *The rigid structure is given by the dual V^* of a representation V. This is the dual vector space with the action*

$$\langle g \triangleright f, v\rangle := \langle f, g^{-1} \triangleright v\rangle$$

for all $g \in G, v \in V, f \in V^*$. ev_V *is simply the pairing between* V^* *and* V *while* $\mathrm{coev}_V : 1 \mapsto \sum_i v_i \otimes f^i$ *where* $\{v_i\}$ *is some basis of* V *and* $\{f^i\}$ *the corresponding dual basis of* V^*.

- *The symmetric structure is given by the trivial braiding*

$$\psi_{V,W}(v \otimes w) = w \otimes v.$$

The simple objects in $\mathcal{R}(G)$ *are the irreducible representations of* G.

We now have the diagrammatic formalism of Section 2.2 at our disposal for group representations and their intertwiners.

3.1.2. Representative functions

We shall be particularly interested in the diagrammatic representation of functions on the group considered as representations. We discuss this in the following.

Let $\mathcal{C}_{\mathrm{alg}}(G)$ denote the complex valued representative functions on G. These are the functions that arise as matrix elements of finite-dimensional complex representations of G. That is, any representative function is of the form

$$g \mapsto \langle \phi, \rho_V(g)v \rangle, \tag{3.1}$$

where V is some finite-dimensional representation, ρ_V denotes the representation matrix and $v \in V, \phi \in V^*$. We can thus identify the function with the vector $\phi \otimes v$ in $V^* \otimes V$. The sum of two representative functions is again a representative function by the identity

$$\langle \phi, \rho_V(g)v \rangle + \langle \phi', \rho_{V'}(g)v' \rangle = \langle \phi + \phi', \rho_{V \oplus V'}(g)(v + v') \rangle \tag{3.2}$$

for the direct sum of representations. Similarly for the product

$$\langle \phi, \rho_V(g)v \rangle \langle \phi', \rho_{V'}(g)v' \rangle = \langle \phi \otimes \phi', \rho_{V \otimes V'}(g)(v \otimes v') \rangle \tag{3.3}$$

by the tensor product of representations.

Consider the action of G on its algebra of functions by conjugation as

$$(g \triangleright f)(h) := f(g^{-1}hg). \tag{3.4}$$

As we will see in Section 5.1 this action is intimately related to gauge transformations in LGT. For a representative function we have the identity

$$(h \triangleright (\phi \otimes v))(g) = (h \triangleright \phi \otimes h \triangleright v)(g) = (\phi \otimes v)(h^{-1}gh). \tag{3.5}$$

That is, this action by conjugation is just the same thing as the action on $V^* \otimes V$ considered as a tensor product of representations. Consequently, we can denote a representative function diagrammatically by a double line, one for V and one for V^* (see Fig. 3.1a). In the following we consider arbitrary elements of $V^* \otimes V$ as representative functions so that besides the addition by direct sum (3.2) we also have the vector addition inside $V^* \otimes V$. By definition, the evaluation of a function at the group identity is just the evaluation of the pairing (see Fig. 3.1b). As the multiplication is given by the tensor product (3.3) it can be diagrammatically represented as in Fig. 3.1c.

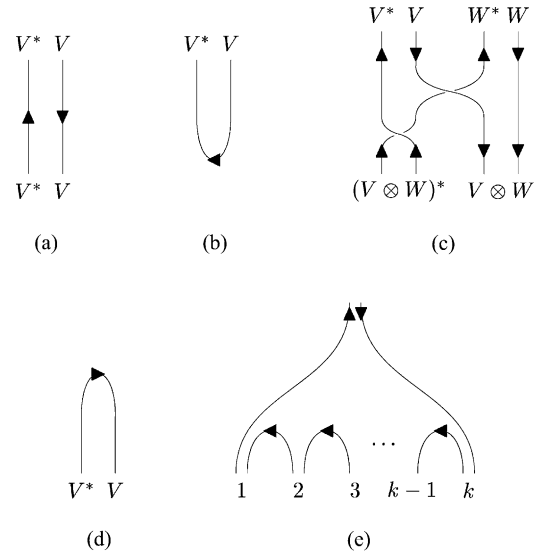

Fig. 3.1. (a) Double line diagram for representative function; (b) evaluation at the group identity; (c) multiplication of representative functions; (d) a character; (e) expansion of a representative function on a product of group elements.

A type of function that is of particular importance in LGT is the character χ_V of a representation V. As an element of $V^* \otimes V$ it is

$$\chi_V = \sum_n \phi_n \otimes v_n, \tag{3.6}$$

where $\{v_i\}$ denotes a basis of V and $\{\phi_i\}$ a dual basis of V^*. Diagrammatically, this is an (arrow-reversed) coevaluation (see Fig. 3.1d). The invariance of a character under conjugation is reflected by the fact that its diagram is closed to the top. Note that the constant function with value 1 is the character for the trivial representation.

Evaluating a representative function on a product of group elements yields the expansion

$$(\phi \otimes v)(g_1 \cdots g_k) = \sum_{n_1,\ldots,n_{k-1}} (\phi \otimes v_{n_1})(g_1)(\phi_{n_1} \otimes v_{n_2})(g_2) \cdots (\phi_{n_{k-1}} \otimes v)(g_k). \tag{3.7}$$

Diagrammatically this expansion is the insertion of coevaluation diagrams (see Fig. 3.1e).

3.1.3. Integration and semisimplicity

If all finite-dimensional representations of G are completely reducible the category $\mathcal{R}(G)$ is semisimple and a normalized bi-invariant integral in the following sense exists.

Definition 3.2. A normalized bi-invariant integral on $\mathcal{C}_{\text{alg}}(G)$ is a map $\int : \mathcal{C}_{\text{alg}}(G) \to \mathbb{C}$ denoted $f \mapsto \int \mathrm{d}g\, f(g)$ such that

$$\int \mathrm{d}g\, f(gh) = \int \mathrm{d}g\, f(hg) = \int \mathrm{d}g\, f(g) \quad \forall h \in G \text{ and } \int \mathrm{d}g = 1.$$

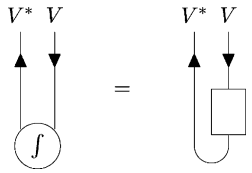

Fig. 3.2. Diagrammatic identity for the integral.

Furthermore, this integral precisely defines the family of morphisms T of Proposition 2.12 in the following way.

Proposition 3.3. *For a representation V the intertwiner $T_V : V \to V$ of Proposition 2.12 is given by the bi-invariant normalized integral as*

$$T_V : v \mapsto \int \mathrm{d}g\, \rho_V(g)v.$$

Thus, the integral of a representative function is

$$\int \mathrm{d}g \langle \phi, \rho_V(g)v\rangle = \langle \phi, T_V(v)\rangle. \tag{3.8}$$

Translating this formula into a diagram yields the identity shown in Fig. 3.2. By combining this with Fig. 3.1c we obtain Fig. 3.3 as the diagrammatic representation of taking the integral of a product of functions.

Two types of groups giving rise to semisimple representation categories are of particular interest: compact Lie groups and finite groups.

Proposition 3.4 (Peter–Weyl decomposition). *Let G be a compact Lie group or a finite group. Then, $\mathcal{R}(G)$ is semisimple and the algebra of representative functions on G has a decomposition*

$$\mathcal{C}_{\mathrm{alg}}(G) \cong \bigoplus_V (V^* \otimes V),$$

where the direct sum runs over all irreducible representations V of G. The isomorphism is an isomorphism as representations of $G \times G$ with the action $((g, g') \triangleright f)(h) = f(g^{-1}hg')$ on the left hand side and the canonical action on the right hand side.

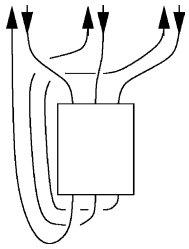

Fig. 3.3. The integral of a product of functions.

The unique normalized bi-invariant integral $\int : \mathcal{C}_{\mathrm{alg}}(G) \to \mathbb{C}$ *is given by the projection*

$$\bigoplus_V (V^* \otimes V) \to \mathbf{1}^* \otimes \mathbf{1} \cong \mathbb{C},$$

where $\mathbf{1}$ *denotes the trivial representation.*

In the Lie group case the representative functions are dense in the L^2*-functions of* G*, to which the integral* (*Haar measure*) *extends.*

In the finite group case the integral can be expressed through a sum

$$\int \mathrm{d}g\, f(g) = \frac{1}{|G|} \sum_{g \in G} f(g),$$

where $|G|$ *denotes the order of* G*.*

3.2. Hopf algebras and quantum groups

Hopf algebras can be considered as generalizations of groups in the sense that they are "noncommutative algebras of functions". Hence the name *quantum groups*. The coproduct thereby encodes the "group structure". We consider Hopf algebras with various amounts of additional structure so that their respective representation theory gives rise to all the different types of categories we are interested in here. See [25] for a general reference covering most of the relevant cases. Spherical Hopf algebras are considered in [20].

We use here the point of view that representations are comodules. This is precisely in the spirit of "noncommutative function algebras" and indeed, as we shall see below, a group is then just (equivalent to) a certain Hopf algebra. This is also the right point of view for supergroups (see, e.g. [26]). Examples of Hopf algebras giving rise to nonsymmetric categories are then the q-deformations of simple Lie groups. Dually, one can consider modules as representations. This corresponds then to Hopf algebras generalizing universal enveloping algebras. However, this implies the loss of "global structure" of the group. But as this point of view is more frequently employed in the literature, many of our definitions have a "co" in them. In the case of finite-dimensional Hopf algebras both points of view are completely equivalent.

We use the notation $\Delta, \epsilon, \mathrm{S}$ for coproduct, counit and antipode of a Hopf algebra. We use Sweedler's notation (with implicit summation) $\Delta a = a_{(1)} \otimes a_{(2)}$ for coproducts and a similar notation $v \mapsto v_{(\underline{1})} \otimes v_{(2)}$ for right coactions.

3.2.1. Representation categories

Definition 3.5. Let H be a Hopf algebra and $\omega : H \to \mathbb{C}$ a convolution-invertible map such that

$$\omega(ab) = \omega(a)\omega(b), \qquad \mathrm{S}^2 a = \omega(a_{(1)}) a_{(2)} \omega^{-1}(a_{(3)})$$

for all $a, b \in H$. We call (H, ω) a *copivotal Hopf algebra*.

Definition 3.6. Let (H, ω) be a copivotal Hopf algebra. It is called a *cospherical Hopf algebra* if for all right H-comodules $\beta : V \to V \otimes H$ and all comodule maps $\theta : V \to V$ the equality

$$\mathrm{tr}((\mathrm{id}_V \otimes \omega) \circ \beta \circ \theta) = \mathrm{tr}((\mathrm{id}_V \otimes \omega^{-1}) \circ \beta \circ \theta)$$

holds.

Definition 3.7. A *coquasitriangular structure* on a Hopf algebra H is a convolution-invertible map $\mathcal{R} : H \otimes H \to \mathbb{C}$ so that

$$\mathcal{R}(ab \otimes c) = \mathcal{R}(a \otimes c_{(1)})\mathcal{R}(b \otimes c_{(2)}), \qquad \mathcal{R}(a \otimes bc) = \mathcal{R}(a_{(1)} \otimes c)\mathcal{R}(a_{(2)} \otimes b),$$
$$b_{(1)}a_{(1)}\mathcal{R}(a_{(2)} \otimes b_{(2)}) = \mathcal{R}(a_{(1)} \otimes b_{(1)})a_{(2)}b_{(2)}$$

for all $a, b, c \in H$. A pair $(H, \mathcal{R})$ is called a *coquasitriangular Hopf algebra*.

Definition 3.8. A *ribbon form* on a coquasitriangular Hopf algebra $(H, \mathcal{R})$ is a map $\nu : H \to \mathbb{C}$ such that

$$\nu(ab) = \mathcal{R}^{-1}(a_{(1)} \otimes b_{(1)})\mathcal{R}^{-1}(b_{(2)} \otimes a_{(2)})\nu(a_{(3)})\nu(b_{(3)}),$$
$$\nu(1) = 1, \qquad \nu(\mathrm{S}a) = \nu(a), \qquad \nu(a_{(1)})a_{(2)} = a_{(1)}\nu(a_{(2)})$$

for all $a, b \in H$. A triple $(H, \mathcal{R}, \nu)$ is called a *coribbon Hopf algebra*.

Lemma 3.9. *A coribbon Hopf algebra is a cospherical Hopf algebra by setting* $\omega(v) := \mathcal{R}^{-1}(\mathrm{S}v_{(1)} \otimes v_{(2)})\nu(v_{(3)})$.

Definition 3.10. A *cotriangular structure* on a Hopf algebra H is coquasitriangular structure satisfying the extra property

$$\mathcal{R}(a \otimes b) = \mathcal{R}^{-1}(b \otimes a)$$

for all $a, b \in H$. A pair $(H, \mathcal{R})$ is called a *cotriangular Hopf algebra*.

Lemma 3.11. *A cotriangular Hopf algebra is a coribbon Hopf algebra by choosing* $\nu := \epsilon$.

Proposition 3.12. *The category* $\mathcal{M}^H$ *of finite-dimensional* (*right*) *comodules of a Hopf algebra H is a rigid monoidal category in the following way*:

- *The monoidal structure is given by the tensor product of comodules. Thus, for two comodules V, W we have a comodule structure on* $V \otimes W$ *via*

  $$v \otimes w \mapsto v_{(\underline{1})} \otimes w_{(\underline{1})} \otimes v_{(2)}w_{(2)}.$$

  The unit object **1** *is the one-dimensional trivial comodule* $v \mapsto v \otimes 1$.
- *The rigid structure is given by the definition of the dual* V^* *of a comodule V. This is the dual vector space with the coaction*

  $$f \mapsto f_{(\underline{1})} \otimes f_{(2)} \quad \textit{such that } \langle f_{(\underline{1})}, v\rangle f_{(2)} = \langle f, v_{(\underline{1})}\rangle \mathrm{S}v_{(2)}$$

for all $v \in V$, $f \in V^*$. ev_V is simply the pairing between V^* and V while $\mathrm{coev}_V : 1 \mapsto \sum_i v_i \otimes f^i$ where $\{v_i\}$ is some basis of V and $\{f^i\}$ the corresponding dual basis of V^*.

- *If H is copivotal/cospherical, then $\mathcal{M}^H$ is a pivotal/spherical category by defining $\tau_V : V \to V^{**}$ for an object V as*

$$\tau_V : v \mapsto v_{(\underline{1})}\omega(v_{(2)}),$$

where V and V^{**} are identified canonically as vector spaces and the coaction is the one on V.

- *If H is coribbon, then $\mathcal{M}^H$ is a ribbon category with braiding*

$$\psi_{V,W}(v \otimes w) = w_{(\underline{1})} \otimes v_{(\underline{1})}\mathcal{R}(v_{(2)} \otimes w_{(2)})$$

and twist

$$\nu_V : v \mapsto v_{(\underline{1})}\nu(v_{(2)}).$$

- *If H is cotriangular, then the category is symmetric with the braiding obtained as*

$$\psi_{V,W}(v \otimes w) = w_{(\underline{1})} \otimes v_{(\underline{1})}\mathcal{R}(v_{(2)} \otimes w_{(2)}).$$

To see how the group case is manifestly a special case of the cotriangular Hopf algebra case note the following fact.

Proposition 3.13. *Let G be a group. Then $\mathcal{C}_{\mathrm{alg}}(G)$ is naturally a commutative Hopf algebra. The coproduct is given by the map*

$$V^* \otimes V \to (V^* \otimes V) \otimes (V^* \otimes V) : \phi \otimes v \mapsto \sum_n (\phi \otimes v_n) \otimes (\phi_n \otimes v)$$

and the antipode is given by $V^* \otimes V \to V \otimes V^* : \phi \otimes v \mapsto v \otimes \phi$, using that canonically $V^{**} \cong V$ as representations.

Furthermore, a finite-dimensional representation of G is canonically the same thing as a finite-dimensional comodule of $\mathcal{C}_{\mathrm{alg}}(G)$ and vice versa by the coaction

$$V \to V \otimes (V^* \otimes V) : v \mapsto \sum_n v_n \otimes (\phi_n \otimes v).$$

If $\mathcal{C}_{\mathrm{alg}}(G)$ is equipped with the trivial cotriangular structure $\mathcal{R} = \epsilon \otimes \epsilon$, then $(H, \mathcal{R})$ can be said to correspond to G in the sense that $\mathcal{M}^H$ is identical to $\mathcal{R}(G)$.

The natural definition of a supergroup in view of the above proposition is that of $\mathbb{Z}_2$-graded commutative Hopf algebra. The elements of the Hopf algebra play the role now of "functions on the supergroup". A $\mathbb{Z}_2$-graded Hopf algebra satisfies the same axioms as a Hopf algebra, except for the compatibility of product and coproduct which is modified to

$$\Delta(ab) = (-1)^{|a_{(2)}||b_{(1)}|}a_{(1)}b_{(1)} \otimes a_{(2)}b_{(2)}. \tag{3.9}$$

$\mathbb{Z}_2$-graded commutativity means then $ab = (-1)^{|a||b|}ba$. To a $\mathbb{Z}_2$-graded commutative Hopf algebra corresponds precisely a cotriangular Hopf algebra which is obtained from the former one by "bosonization" and has exactly the same representation theory [25].

However, the cotriangular Hopf algebra point of view is more general and superior from a physical point of view as it allows the algebraic implementation of spin-statistics relations. In particular, this is relevant for the formulation of supersymmetric theories. The convenient definition of supergroup in our context is thus that of a cotriangular Hopf algebra H equipped with a surjection to the Hopf algebra of functions on $\mathbb{Z}_2$ with nontrivial braiding (see [26] for details). The cotriangular structure encodes the $\mathbb{Z}_2$-grading on the representations (comodules) as

$$\psi_{V,W}(v \otimes w) = (-1)^{|v||w|} w \otimes v. \tag{3.10}$$

3.2.2. Representative functions

We now consider how elements of a Hopf algebra can be dealt with in a similar manner as representative functions on a group.

Let H be a Hopf algebra. For a finite-dimensional vector space V the space $V^* \otimes V$ has canonically the structure of a coalgebra by the coaction

$$\Delta\phi \otimes v = \sum_n (\phi \otimes v_n) \otimes (\phi_n \otimes v) \quad \text{and counit } \epsilon(\phi \otimes v) = \langle \phi, v \rangle. \tag{3.11}$$

Given a finite-dimensional comodule V of H we obtain a map of coalgebras $V^* \otimes V \to H$ via

$$\phi \otimes v \mapsto \langle \phi, v_{(\underline{1})} \rangle v_{(2)}. \tag{3.12}$$

In fact, any element of H is in the image of such a map. To see this, consider H as a right comodule under itself by the coproduct. Any given $h \in H$ is contained in some finite-dimensional subcomodule $V \subseteq H$. Choose $\phi \in V^*$ such that $\phi(v) = \epsilon(v)$ for any $v \in V$. Then, $\phi \otimes h \mapsto h$ under the above map.

Therefore, similarly to the group case, we can represent elements of H by double line diagrams. The coaction of H on itself implicit in this notation is now the right adjoint coaction $h \mapsto h_{(2)} \otimes (\mathrm{S}h_{(1)})h_{(3)}$. The diagram for the counit is just the evaluation. The diagram for the coproduct is obtained by inserting coevaluations as follows from (3.11). To make the analogy with the group case complete, we can define a character by the (arrow-reversed) coevaluation diagram. We obtain then exactly the diagrams (a), (b), (d) and (e) of Fig. 3.1. Note that the counit expresses evaluation at the identity while the coproduct expresses evaluation on a product of group elements in the group case.

3.2.3. Integration and semisimplicity

Proceeding in an analogous way as for groups, we introduce in the semisimple case the integral which defines the T-morphism and its diagrammatic representation.

Definition 3.14. Let H be a Hopf algebra. A bi-invariant normalized integral on H is a map $\int : H \to \mathbb{C}$ such that

$$h_{(1)} \int h_{(2)} = \left(\int h_{(1)} \right) h_{(2)} = 1 \int h \quad \forall h \in H \quad \text{and} \quad \int 1 = 1.$$

Note in particular that Definition 3.2 is the special case of Definition 3.14 for $H = \mathcal{C}_{\mathrm{alg}}(G)$.

Proposition 3.15. *For an object V the intertwiner $T_V : V \to V$ of* Proposition 2.12 *is given by the bi-invariant normalized integral as*

$$T_V : v \mapsto v_{(\underline{1})} \int v_{(2)}.$$

Note that in the double line diagrammatics considered above we obtain the identity of Fig. 3.2 as from (3.12) we have

$$\int (\phi \otimes v) \mapsto \langle \phi, v_{(\underline{1})} \rangle \int v_{(2)} = \langle \phi, T_V(v) \rangle. \tag{3.13}$$

The generalization of a compact Lie group or finite group is a cosemisimple Hopf algebra. That is, a Hopf algebra which is as a coalgebra a direct sum of simple coalgebras. The structure of cosemisimple Hopf algebras is captured by the following proposition.

Proposition 3.16 (Peter–Weyl decomposition). *Let H be a cosemisimple Hopf algebra. Then $\mathcal{M}^H$ is semisimple and the following isomorphism of coalgebras holds*

$$H \cong \bigoplus_V (V^* \otimes V),$$

where the direct sum runs over all simple (*right*) *comodules V of H. $V^* \otimes V$ is a simple coalgebra as above with the isomorphism as given there.*

The unique normalized left and right invariant integral $\int : H \to \mathbb{C}$ is given by the projection

$$\oplus_V (V^* \otimes V) \to \mathbf{1}^* \otimes \mathbf{1} \cong \mathbb{C},$$

where **1** *denotes the trivial comodule.*

4. The partition function

We start by fixing some terminology. In the following, *complex* means finite CW-complex (see, e.g. [27]). A *lattice* means a finite combinatorial 2-complex. For a lattice we use the terms *vertex*, *edge*, *face* to denote 0-, 1-, and 2-cells, respectively. We use the term *cellular manifold* to denote a compact manifold together with a cellular decomposition as a finite CW-complex. The *lattice associated with a cellular manifold* means the 2-skeleton of the dual complex. A standard reference for LGT is [28].

4.1. Ordinary and symmetric LGT

It is well known that LGT admits a spin foam formulation [2]. In [3] the corresponding transformation was explicitly performed on a hypercubic lattice and it was shown that the new formulation is strong–weak dual to the original one. We perform here a generalization of this transformation employing the categorial and diagrammatic language introduced in the previous sections. This allows us to generalize LGT to arbitrary semisimple symmetric categories (e.g., including supersymmetric LGT).

Let L be a lattice and G a compact Lie group or finite group. We might think of L as arising as the lattice associated with a cellular manifold M. We equip the faces of L with arbitrary but fixed orientations. Recall that in LGT a group element g is attached to every edge (with a given orientation). The action S is the sum over all faces f of a function σ evaluated on the product of group elements attached to the edges e bounding the face f (cyclically ordered by the orientation of the face). We write this as

$$S = \sum_f \sigma\left(\prod_{e\in\partial f} g_e\right). \tag{4.1}$$

The function σ is required to be invariant under conjugation (3.4) and to satisfy $\sigma(g^{-1}) = \sigma(g)$. The conjugation invariance ensures that it does not matter at which vertex we start taking the product over group elements, only the cyclic order is relevant. The partition function reads

$$\mathcal{Z} = \int \left(\prod_e \mathrm{d}g_e\right) \mathrm{e}^{-S} = \int \left(\prod_e \mathrm{d}g_e\right) \prod_f \mathrm{e}^{-\sigma(\prod_{e\in\partial f} g_e)}. \tag{4.2}$$

As $\mathrm{e}^{-\sigma}$ is itself invariant under conjugation it can be expanded as

$$\mathrm{e}^{-\sigma} = \sum_V \alpha_V \chi_V, \tag{4.3}$$

where the sum runs over the irreducible representations V of G and χ_V is the character of the representation V. Since $\mathrm{e}^{-\sigma(g^{-1})} = \mathrm{e}^{-\sigma(g)}$ we have $\alpha_{V^*} = \alpha_V$ because of $\chi_V(g^{-1}) = \chi_{V^*}(g)$. Thus

$$\mathcal{Z} = \int \left(\prod_e \mathrm{d}g_e\right) \prod_f \sum_V \alpha_V \chi_V \left(\prod_{e\in f} g_e\right) = \sum_{V_f} \left(\prod_f \alpha_{V_f}\right) \mathcal{Z}_{V_f} \tag{4.4}$$

with

$$\mathcal{Z}_{V_f} := \int \left(\prod_e \mathrm{d}g_e\right) \prod_f \chi_{V_f} \left(\prod_{e\in f} g_e\right), \tag{4.5}$$

where V_f denotes an assignment of an irreducible representation V to every face f and we sum over all such assignments.

The next step is to expand the characters into functions (i.e., matrix elements) taking as values the individual group elements attached to the edges. Then, for each edge all the functions taking the attached group element as their value are multiplied and integrated. Instead of proceeding formally we perform these manipulations diagrammatically. This leads to a diagrammatic representation of the partition function. The obtained diagram is naturally embedded into the lattice and into the manifold (if the lattice arises from one).

To represent functions on the group diagrammatically we utilize the diagrammatic language introduced in the previous sections. Notably, we consider an action of the gauge

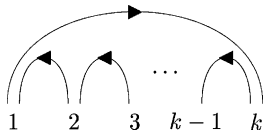

Fig. 4.1. The diagram of a character evaluated on a product of group elements.

group by conjugation (3.4). As we shall discuss in Section 5.1 this precisely encodes gauge transformations.

As introduced in Section 3.1.2 a character χ_V is represented by a coevaluation diagram (Fig. 3.1d) due to its decomposition (3.6) as basis and dual basis over the representation V. Thus, from (4.5) we obtain one such diagram for each face. As each character is evaluated on the product of group elements attached to the edges bounding the face, we expand it into functions of the individual group elements. This means attaching the diagram of Fig. 3.1e to each character diagram. We obtain a diagram as shown in Fig. 4.1 for every face whereby the double lines correspond to the edges bounding the face. Thus, we can embed the diagram for each face into the face as shown in Fig. 4.2. The direction of the arrows is chosen in correspondence to the orientation of the face. Proceeding in this way for each face, all double lines denoting functions that take the group value for a given edge meet in this edge (see Fig. 4.3).

To integrate the product of functions taking their value at a given edge as prescribed by (4.5) we insert the appropriate diagram (Fig. 3.3) at each edge, connecting the double lines. For ease of notation, we now draw the lines in each face such that they run close to the boundary. We draw the T-projections (the unlabeled coupon in Fig. 3.3) arising in the integration as (hyper)-cylinders with axis given by the edges. Proceeding thus for every edge we arrive at a diagram embedded in the lattice as shown in Fig. 4.4.

As this diagram is closed it represents an intertwiner $\mathbf{1} \to \mathbf{1}$ and thus a complex number which is exactly $\mathcal{Z}_{V_f}$ in (4.5). Thus, the partition function is the sum over this diagram with all possible assignments of irreducible representations to the faces with weights given by the α_V. Note that this is independent of the choice of orientations for the faces. Indeed, changing the orientation of a face leads to the same partition function, except that α_V and α_{V^*} for this face are interchanged. However, they are equal by assumption.

Since the diagram resembles an arrangement of wires and cables we denote the lines representing the characters as *wires* and the (hyper)-cylinders representing the T-projectors

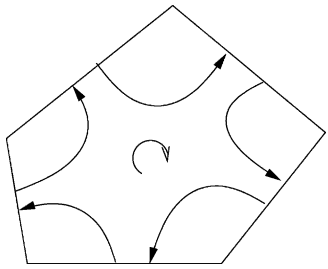

Fig. 4.2. The diagram of a character embedded into a face.

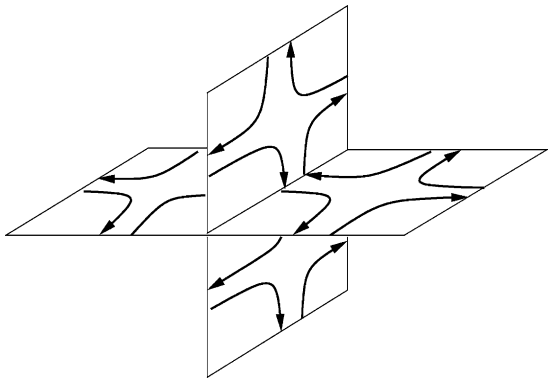

Fig. 4.3. The character diagrams embedded into a three-dimensional cubic lattice. In this example four double lines meet at each edge.

as *cables*. When referring to an individual wire we usually mean all the lines lying in a given face as they come from the same character. They carry the same representation label and arrow orientation and we can imagine them being connected inside the cables.

Let us remark that the arrows on the wires in a given cable do not necessarily all point in the same direction (as in Fig. 3.3). This indeed must be so as those functions originating from faces with opposite orientation with respect to the one in which the edge carries the group value g are evaluated at g^{-1} instead. The relative directions of the arrows encode this information.

Starting from the lattice the diagram is obtained in a very simple way. Put one wire into each face running close to the boundary. Give each wire an arrow according to the orientation of the face and the representation label of the face. Then, for each edge, put a cable in the middle of the edge, around the wires that run along the edge. We refer to the

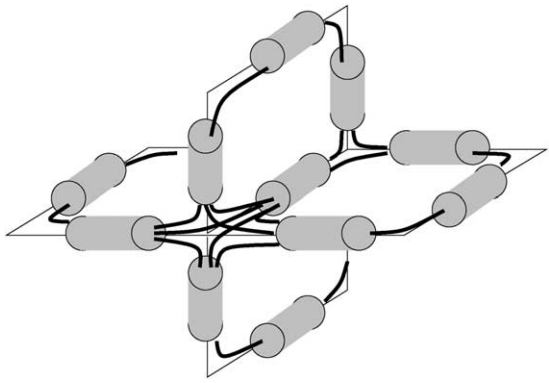

Fig. 4.4. The circuit diagram obtained after inserting the integrals. This example shows wires (thick lines) and cables (gray cylinders) in a piece of three-dimensional cubic lattice. The arrows on the wires are omitted.

diagram as the *circuit diagram* associated to the lattice. Note that it is a spin network in the sense of Section 2.2.

Strictly speaking, we have in Section 2.2 only defined how to evaluate a diagram that can be written on a "piece of paper", i.e., in the plane. However, as discussed there, the value of the diagram only depends on the combinatorial data, i.e., which piece of wire is connected to which side of which cable and with which arrow. This information is completely determined by the lattice. Any way of writing the diagram on a piece of paper (we refer to this as *projection*) will give the same result.

Changing our point of view, we can now consider the obtained representation of the partition function as a definition and thereby extend it to arbitrary semisimple symmetric categories.

Definition 4.1. Let $\mathcal{C}$ be a semisimple symmetric category. Let $\{\alpha_V\}$ be an assignment of a complex number to each isomorphism class of simple object V such that $\alpha_{V^*} = \alpha_V$. These are called *weights*. Let L be a lattice, possibly associated with a cellular manifold M. This defines an *LGT* as follows.

For any choice of orientation and labeling V_f with an equivalence class of simple objects for each face we define $\mathcal{Z}_{V_f}$ to be the value of the circuit diagram constructed above. We call

$$\mathcal{Z} := \sum_{V_f} \left(\prod_f \alpha_{V_f} \right) \mathcal{Z}_{V_f}$$

the *partition function*, where the sum runs over all possible labelings. This does not depend on the chosen orientations of the faces.

By the above derivation, this definition agrees with ordinary LGT in the case where $\mathcal{C} = \mathcal{R}(G)$. Note that as $\mathcal{Z}_{V_f}$ is finite by construction, $\mathcal{Z}$ is manifestly finite if $\mathcal{C}$ has only finitely many isomorphism classes of simple objects. However, it might be infinite in general. In ordinary LGT it is finite by construction in spite of the sum over labelings being infinite for a Lie group.

4.2. Nonsymmetric LGT

In the present section we extend our definition of LGT to nonsymmetric categories. This turns out to require topological information beyond the lattice. That is, we need to start with a cellular manifold and the admissible type of nonsymmetric category depends on the dimension of the manifold. Also the manifold is now required to be orientable. The type of category admissible is the same as for state sum invariants of Turaev–Viro type, namely spherical in three dimensions [15] and ribbon in four dimensions [17]. This is not surprising as these invariants arise indeed as special cases of our construction. This will be discussed in Section 8.2. In two dimensions we can use pivotal categories.

That the circuit diagram constructed in the previous section cannot alone be used to define a partition function is clear. For pivotal, spherical and ribbon categories the value of the

diagram depends on the way it is projected onto the plane and not just on its combinatorial data. This extra data is extracted from topological information about the cellular manifold.

Let M be an oriented cellular 2-manifold and consider its circuit diagram. The only obstruction to its direct evaluation is the non-planar topology of M. Instead, we cut out all the 2-cells (with the wire pieces) and project them separately onto the plane, using the orientation of M. This cuts all the cables in half. Now, we reconnect the cables with T-coupons, thereby possibly introducing crossings. The "layout" for these T-coupons is irrelevant, however, as they can arbitrarily cross (Fig. 2.7) and "twist" (Fig. 2.8). Thus, we obtain a well-defined morphism $\mathbf{1} \to \mathbf{1}$ (which is a complex number) in the pivotal category.

The situation in higher dimensions is more involved and we start by outlining the n-dimensional setting before specializing to $n = 3$ and 4.

Let M be an oriented cellular manifold of dimension n and L the associated lattice, embedded into M. The key idea is to embed the circuit diagram into the $n-1$-dimensional subcomplex of M. Again we choose an arbitrary orientation for each face (or equivalently $(n-2)$-cell).

Instead of embedding the wires arbitrarily into the faces of the lattice we put them on the intersections of these faces with the $(n-1)$-cells. Thus, every $(n-1)$-cell carries two pieces of wire for each face that it intersects. The two correspond to the two (not necessarily distinct) n-cells that are bounded by the $(n-1)$-cell and they lie on top of each other. (It might be helpful to imagine the wires to be slightly displaced into the respective n-cells.) Each piece of wire carries the object label and direction inherited from the face. The wire pieces end precisely at the intersections of the $(n-1)$-cells with the edges. Now we put a "small" $(n-2)$-sphere around each intersection of an $(n-1)$-cell with an edge, into the $(n-1)$-cell. We let the wire pieces end on those $(n-2)$-spheres instead of the edges. The $(n-1)$-balls bounded by these $(n-2)$-spheres are to be thought of as the (infinitely shortened) cables (see Fig. 4.5 for an illustration).

By definition of a CW-complex, we can think of the boundary of an n-cell always as an $(n-1)$-sphere with some of its constituent $(n-1)$-cells possibly identified. It is natural to consider this $(n-1)$-sphere (before identification) as carrying the wire pieces belonging to the n-cell. The idea for evaluating the circuit diagram is now to "cut out" the $(n-1)$-sphere for each n-cell with its wire pieces and to project it onto the plane to define (almost) a morphism (upon labeling) (see Fig. 4.6). Note that each $(n-1)$-cell occurs twice in the projections, once for the n-cell that it bounds on each side. (These n-cells might be

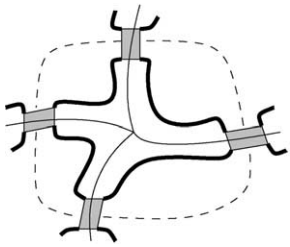

Fig. 4.5. The circuit diagram embedded into the $(n-1)$-complex. The thin lines are the $(n-1)$-cells. The gray boxes are the cables. The thick lines are the wires, for illustration slightly displaced from the boundaries into the n-cells. The face dual to the $(n-2)$-cell at the meeting point in the center is indicated by a dashed line.

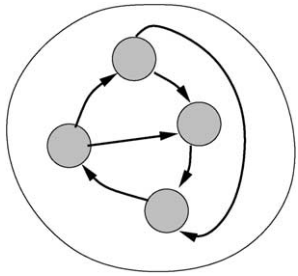

Fig. 4.6. The projection of the boundary of an n-cell with wires and cables. The wire pieces end on the boundaries of the cables ($(n-1)$-balls) which are shaded.

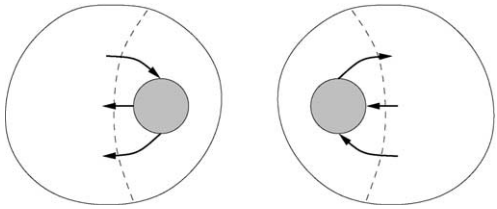

Fig. 4.7. Two projected $(n-1)$-spheres containing the same $(n-1)$-cell. The projections of this $(n-1)$-cell (indicated by the dashed line) are mirror images.

identical leading to the $(n-1)$-cell appearing twice in one projected $(n-1)$-sphere.) Using the orientation in performing the projections the two occurrences of each $(n-1)$-cell agree in the sense of being mirror images (see Fig. 4.7). Then one reconnects all the individual diagrams at the matching (mirror image) cable ends with T-coupons (see Fig. 4.8). We call this the *projected circuit diagram* which (upon labeling) gives rise to a morphism $\mathbf{1} \to \mathbf{1}$ in the relevant category and thus a complex number.

Our description already suggests that the admissible type of category depends on the isotopy properties of the diagrammatics. More precisely, we should have isotopy invariance on S^{n-1}, as this is where the (unconnected) diagrams live. Indeed, this approach can be realized in dimension 3 for spherical categories and in dimension 4 for ribbon categories (compare Table 1). We describe this in the following.

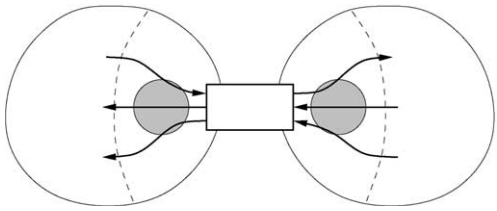

Fig. 4.8. Reconnecting the cable ends (gray disks) by a T-coupon.

4.2.1. Dimension 3—spherical categories

Before projecting, we mark each of the circles that represent the cables at some arbitrary point (not coinciding with the end of a wire piece). Then, to perform the projections, each 2-sphere (bounding a 2-cell) is punctured at some arbitrary point (which does not lie in any of the circles or on any of the wire pieces). Now, each 2-sphere is flattened out and projected onto the plane such that its outside is facing up. In doing so we respect the orientation of M. This ensures that the orientations of the projected 2-spheres all match up in the sense that the two projections of each 2-cell are mirror images. We wish to think of the images of the 2-spheres as diagrams defining (upon labeling with objects) morphisms in the category. For each projected cable end (represented by a circle) we arrange the wires ending there in a line by cutting the circle at the marked point. Now if we could pull these lines to the top or bottom line of the diagram this would (upon labeling) specify a morphism. As this would possibly imply introducing crossings this is not in general possible. Nevertheless, we can connect the corresponding wires lined up at the cable ends by T-coupons. This is because T-coupons are allowed to cross arbitrarily. The emerging diagram is the desired projected circuit diagram. It defines (upon labeling) a morphism $\mathbf{1} \to \mathbf{1}$ in the spherical category and thus a complex number.

We proceed to show the well definedness (invariance under the choices made) of the obtained morphism (for any labeling). For given projections, the morphism is independent on the way the T-coupons are inserted to connect matching cable ends. This is because the T-coupons can cross arbitrarily (Fig. 2.7) and "windings" in the connections are irrelevant (Fig. 2.8). The invariance of the morphism under the way the projections of the 2-spheres are performed (while respecting the orientation) follows precisely from the S^2 isotopy invariance of the diagrammatics. Notably, the invariance under the choice of point at which each boundary 2-sphere is pierced is precisely the identity of Fig. 2.3. Note that a diagram that is bounded only by cables behaves in this sense like a closed diagram. It remains to show the invariance under the choice of marked point for each cable. Moving this point across the end of a wire gives precisely rise to diagrams that are related as the sides of Fig. 2.10. As these are identical invariance follows.

4.2.2. Dimension 4—ribbon categories

We start by turning the wires into ribbons, i.e., equip them with a framing. As we confine the framing to the boundary 3-spheres in which the wires lie this gives indeed rise to ribbons (again inside the 3-spheres). It turns out that one is free to choose the framing as long as it is coherent in the following way. Recall that the wire pieces all occur in pairs (each belonging to one of the two bounded 4-cells) which lie on top of each other. A framing is said to be coherent, if for each piece of wire the corresponding piece of wire has exactly the same framing, but face-side and backside exchanged. Next, we arrange the ribbon wire endings on each of the 2-sphere cables in a line, with the framings pointing along the line, all faces (for each bounded 4-cell) on the same side. We do this while keeping corresponding wire pieces identified (except for their face-side and backside being opposite).

Now, we puncture each of the bounding 3-spheres at a point to identify them with $\mathbb{R}^3$. Hereby we respect the orientation and choose the "outward" direction for all the 3-spheres to be the same in the ambient $\mathbb{R}^4$ (considering the $\mathbb{R}^3$ as a subspace of this). (This is the analog to projecting 2-spheres "face up" in the three-dimensional case.) Then, for each

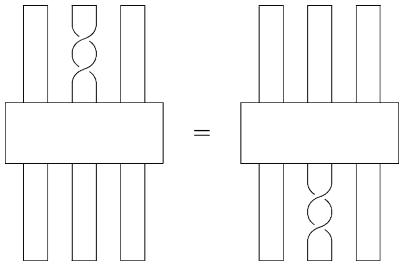

Fig. 4.9. Pulling a twist through a T-coupon.

3-sphere we project the obtained ribbon tangle in $\mathbb{R}^3$ onto the plane. We do this in such a way that the aligned ribbons that end on the 2-spheres (cables) are projected "face up". To let the projections define morphisms (upon labeling) we would need to pull the ribbon ends to the top or bottom line of each diagram. However, we do not need to do that but can proceed to connect the corresponding ribbon ends with T-coupons. The resulting diagram is the desired projected circuit diagram. It defines (upon labeling) a morphism $\mathbf{1} \to \mathbf{1}$ in the category and thus a complex number.

We proceed to show the well definedness (invariance under the choices made) of the obtained morphism (for any labeling). For given projections, the morphism is independent on the way the T-coupons are inserted to connect matching cable ends. This is because the T-coupons can cross arbitrarily (Fig. 2.6g) and "windings" in the connections are irrelevant (Fig. 2.6h). The invariance of the morphism under the way the projections of the 3-spheres are performed (while respecting the orientation) follows precisely from the S^3 (or $\mathbb{R}^3$ which is the same) isotopy invariance of the diagrammatics. For the invariance under the choice of framing we note that a change in the framing for a given piece of wire induces by construction a corresponding change in the corresponding piece of wire. These give rise to additional twists in the projections of this wire piece which appear as mirror images on both sides of the relevant T-coupon. As the T-coupon commutes with any morphism the twists can be pulled "through" to the same side of the T-coupon where they "annihilate" each other (see Fig. 4.9). It remains to show the invariance under the choice of alignment of ribbons for each cable. Any such alignment can be obtained from a given one by inserting an isotopy in a neighborhood of the 2-sphere (cable). In the projections this amounts to inserting a diagram consisting of crossings and twists. This diagram is inserted on both sides of the T-coupon with one being the mirror image of the other. However, as we can pull any morphism (such as the inserted diagram) through a T-coupon, the two mirror images annihilate each other, leaving the total diagram invariant.

4.2.3. Definition of the partition function

We proceed to give the formal definition of LGT for the considered nonsymmetric settings analogous to Definition 4.1.

Definition 4.2. Let $\mathcal{C}$ be a semisimple pivotal category and $n = 2$ or a semisimple spherical category and $n = 3$ or a semisimple ribbon category and $n = 4$. Let $\{\alpha_V\}$ be an assignment

of a complex number to each isomorphism class of simple object V such that $\alpha_{V^*} = \alpha_V$. These are called *weights*. Let M be an oriented cellular manifold of dimension n. This defines an *LGT* as follows.

For any choice of orientation and labeling V_f with an equivalence class of simple objects for each $(n-2)$-cell f we define $\mathcal{Z}_{V_f}$ to be the value of the projected circuit diagram constructed above. We call

$$\mathcal{Z} := \sum_{V_f} \left(\prod_f \alpha_{V_f} \right) \mathcal{Z}_{V_f}$$

the *partition function*, where the sum runs over all possible labelings. This does not depend on the chosen orientations of the $(n-2)$-cells.

The independence of $\mathcal{Z}$ on the chosen orientations follows in the same way as in the symmetric case. This is now due to Lemma 2.4. In the two-dimensional case it would also make sense to induce the orientations of the faces from the orientation of M. Then we can drop the condition $\alpha_V = \alpha_{V^*}$, making $\mathcal{Z}$ possibly dependent on the orientation of M.

5. Gauge symmetry and gauge fixing

In this section we consider how the gauge invariance of LGT manifests itself in the diagrammatic formulation. Then we show how the notion of gauge fixing in conventional LGT translates into the diagrammatic language and generalizes to the symmetric, pivotal, spherical and ribbon settings. Furthermore, it turns out to be related to a topological move between cellular decompositions which is thus an invariance of the partition function.

5.1. Gauge symmetry

Recall that in conventional LGT a gauge transformation is defined by assigning a group element g_v to each vertex v. This changes a configuration (i.e., an assignment of group elements to edges) as follows. For a given edge e the assigned group element h is replaced by $g_{v_1} h g_{v_2}^{-1}$ where v_1 and v_2 are the vertices bounding e. The order of the vertices is determined by the orientation of e.

Consider the LGT action (4.1). The effect of a gauge transformation on the function σ (and thus for the characters in the expansion of its exponential) is precisely an action of the group by conjugation (3.4). Namely, σ is conjugated by the group element assigned by the gauge transformation to the vertex which forms the starting point for the product over group elements which is the argument of σ. Conjugation invariance of σ implies gauge invariance.

In the diagrammatic formulation the gauge invariance is much more implicit. The fact that the diagrams represent intertwiners means that we have an underlying action of the gauge group "everywhere". The fact that a diagram is closed implies invariance. However, we can still specifically identify the original gauge invariance.

For simplicity we consider a gauge transformation that is nontrivial only at one vertex. Deform the (two-dimensionally projected) diagram that defines the partition function such

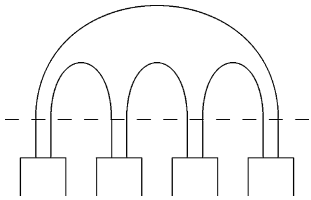

Fig. 5.1. Gauge symmetry at a vertex. Acting with the group at the cut (dashed line) is equivalent to a gauge transformation.

that the considered vertex is at the top with all attached cables leading downward to the remaining diagram (see Fig. 5.1). Then we introduce a horizontal cut in the diagram, just on top of the cables (dashed line). As the diagram above the cut is closed to the top it is invariant. Thus, we can act with a group element g on the tensor product of representations that is represented by the wires crossing the dashed line without changing the value of the diagram. This action is simply an action with g on each tensor factor. As the wire pieces represent functions on the group obtained from the expansion of the characters, the action with g corresponds to an insertion of g into the evaluation of the function. Each piece of wire crosses the dotted line twice corresponding to an insertion of g for each of the two edges connected by the piece of wire. However, the orientation in both cases is opposite (including the arrow, it points upwards at one crossing and downwards at the other). Thus, it corresponds to inserting g on one side and g^{-1} on the other. We recover an ordinary gauge transformation.

So far we have only talked about the case of ordinary group symmetries as only in that case gauge transformations can be defined in the conventional way. However, the statement of gauge symmetry can more generally be considered to lie in the fact that we have a diagrammatic formulation of the partition function. As a diagram determines a morphism in the relevant category it is covariant by construction. This covariance is with respect to a group, a supergroup or a quantum group (Hopf algebra) if the category arises as the category of representations of the respective object.

5.2. Gauge fixing

As we know from conventional LGT we can use its gauge symmetry to remove some of the group integrals in the partition function (4.2). The corresponding group variables can be set to the unit element. We are allowed to do this for the group variables of as many edges as we like, as long as these do not form any closed loop [29].

How is this "gauge fixing" expressed diagrammatically? Looking back at expression (3.8) we see that removing the integral means applying the evaluation without the T-projector. Diagrammatically, the projector diagram is simply removed, i.e., replaced by the identity. In the circuit diagram this means that we can remove cables by exposing the wires without changing the value of the diagram. Conventional LGT tells us that we are allowed to do this as long as the edges for which the attached cables have been removed do not form any closed loop.

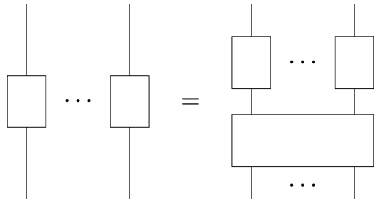

Fig. 5.2. Multiple composition property of T.

As the gauge invariance is contained in the diagrammatic formulation we should be able to derive the gauge fixing directly diagrammatically—without recurrence to conventional LGT. This is indeed the case, as we will show by exploiting the properties of the T-projector (Proposition 2.12 and Fig. 2.6). This generalizes gauge fixing of conventional LGT from the group context to the general symmetric setting as well as to the pivotal, spherical and ribbon settings in the relevant dimensions. We start by deriving the identity that enables the gauge fixing on the purely diagrammatic level. In the ribbon case we assume blackboard framing.

Let us first observe the additional property of T depicted in Fig. 5.2. A tensor product of T-projectors is equal to this same tensor product composed with an overall T-projector. This follows straightforwardly by multiple application of properties (c) and (e) of Fig. 2.6.

Consider now a diagram with T-coupons (which might arise as the projection of a circuit diagram). Draw a closed loop that only intersects T-coupons. By moving the T-coupons around we arrive at a diagram as shown in Fig. 5.3 on the left hand side (for the case of four cables with two wires each). The loop is represented by the dashed line. The part of the diagram between the T-coupons lies inside the dashed box and is indicated by three dots. The rest of the diagram is attached at the top and bottom and lies outside the dashed box.

Now consider the dotted box. Whatever lies inside defines a morphism by construction. Thus, we can apply property (d) of Proposition 2.12 (see Fig. 2.6) to the T-coupon at the

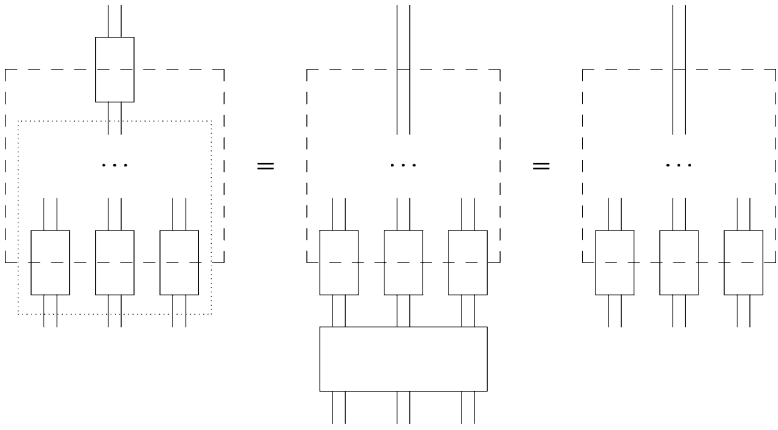

Fig. 5.3. Diagrammatic gauge fixing identity.

top and this morphism. That is to say we can exchange the two. The result is shown in the diagram in the middle of Fig. 5.3. Now, the arrangement of the T-coupons at the bottom resembles the right hand side of Fig. 5.2. That is, we can apply the identity of this figure to arrive at the right hand side diagram of Fig. 5.3. The result of the operation is simply the disappearance of the T-coupon that was originally at the top.

5.3. *n-Cell fusion invariance*

It turns out that gauge fixing is much more than an identity that helps us to simplify diagrams. Assume we are given a diagram that arises as the projection of a circuit diagram for a cellular manifold. Assume further that we obtain a new diagram from the given one by applying a gauge fixing identity (as in Fig. 5.3). Remarkably, it turns out that the new diagram is still a projection of the circuit diagram for the same manifold—but with different cellular decomposition. The process that transforms one cellular decomposition into the other is given by the following definition.

Definition 5.1. Let M be a manifold of dimension n with cellular decomposition $\mathcal{K}$. Let μ be an $(n-1)$-cell in $\mathcal{K}$ which bounds two distinct n-cells σ, σ'. Removing μ, σ and σ' from $\mathcal{K}$ while adding the new n-cell $\sigma'' := \sigma \cup \mu \cup \sigma'$ leads to a new cellular decomposition $\mathcal{K}'$ of M. We call this process the n-cell fusion move.

As a consequence the partition function remains invariant under this move. To proof our claim let us first consider what the n-cell fusion move means for the circuit diagram. In the context of Definition 5.1, the $(n-1)$-cell μ corresponds to an edge of the associated lattice and thus a cable of the circuit diagram which is removed. The wires remain exactly the same however as they correspond to faces and thus $(n-2)$-cells which are not changed. That is, the cellular decompositions $\mathcal{K}$ and $\mathcal{K}'$ have identical circuit diagrams except that in the one for $\mathcal{K}'$ a cable is removed, exposing the wires.

We need to verify that the projections of the circuit diagram are related by a gauge fixing identity as depicted in Fig. 5.3. First, identify the projection of the circuit diagram for $\mathcal{K}$ with the left hand side diagram of Fig. 5.3 as follows. σ is projected to the interior of the dashed box, μ to the top part of the dashed line and σ' above it. The dashed line intersects only cables as it is the projection of the boundary of σ. Thus, the diagrammatic identity can be applied which corresponds to removing the cable that "pierces" μ, as required.

What remains to check is that the diagram obtained by first projecting the circuit diagram and then applying the diagrammatic identity is equivalent to the diagram obtained by first applying the move (changing the circuit diagram) and then projecting. This is obvious if any kind of projection (preserving the combinatorics) is allowed, as for symmetric categories. It is equally obvious in the two-dimensional pivotal case. It is less obvious though for the spherical (three-dimensional) and ribbon (four-dimensional) cases. As in those cases n-cells (more precisely: their boundaries) are projected separately it is sufficient to consider just the projections of (the boundaries of) σ, σ' and σ''. We make use of the fact that the boundaries of σ and σ' share the $(n-1)$-cell μ. Thus, we choose the projections of the boundaries of σ and σ' such that the projections of μ are identical as mirror images (as the orientation is reversed). Furthermore, we make sure that the cable ending in μ lies near the boundary

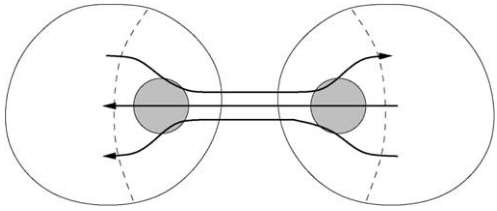

Fig. 5.4. Applying the gauge fixing to the projection, removing a T-coupon (cable).

of each projection, i.e., there is no wire between the cable ending and the boundary of the projection. (In the spherical three-dimensional case this is achieved by choosing the point piercing the boundary 2-spheres close to this cable. In the ribbon four-dimensional case this is simply achieved by an appropriate three-dimensional isotopy.) Also we make sure in the four-dimensional ribbon case that there are no crossings inside the projection of μ, and that blackboard framing applies there (again by isotopy). The projection we obtain is illustrated by Fig. 4.7, and after inserting the T-coupon by Fig. 4.8. It is now clear that removing the T-coupon from the lines that connect the two projected cells (Fig. 5.4) we can pull the projections together (until the dashed lines coincide) to obtain precisely a projection of (the boundary of) σ'' (see Fig. 5.5). This completes the proof.

Theorem 5.2. *Let M be a manifold of dimension n and $\mathcal{K}$, $\mathcal{K}'$ cellular decompositions of M which are related by a sequence of n-cell fusion moves. Then, the value of the circuit diagram in a symmetric* (*or ribbon if $n = 4$, or spherical if $n = 3$, or pivotal if $n = 2$*) *category for a given labeling and choice of orientation of $(n-2)$-cells is the same for $\mathcal{K}$ and $\mathcal{K}'$. In particular, the partition function for both is the same.*

We turn now to the question what the analog of the "no-loop" condition for the gauge fixed edges of conventional LGT is. The only situation that prevents us from removing a cable and fusing the two n-cells that it connects is when these n-cells are actually identical. In that case the dual edge corresponding to the cable forms indeed a closed loop and we are not allowed to gauge fix it. Conversely, given a set of dual edges that forms a loop, we cannot remove all of the cables belonging to it. This is because just before removing the last cable, the path formed by the gauge fixed edges would lie completely inside one n-cell. Thus, the remaining cable would belong to an $(n-1)$-cell which bounds this one n-cell on both sides and therefore cannot be removed by n-cell fusion.

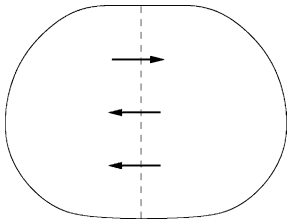

Fig. 5.5. Pulling the projected diagram together, so that a projection of the fused n-cell results.

In the symmetric category case we do not need to think of the lattice as arising from a cellular complex. In that case we can express the gauge fixing move directly in terms of the lattice. It corresponds to removing one edge by identifying all its points so that its two bounding vertices become one. This is only allowed if these two bounding vertices are distinct.

6. Observables

The standard observables of conventional LGT are Wilson loops or, more generally (embedded) spin networks. A Wilson loop L is a subset of edges of the lattice that form a closed loop, carry a consistent orientation, and it has attached the label of an irreducible representation. The partition function (4.2) with a Wilson loop inserted takes the form

$$\mathcal{Z}[L] = \int \left(\prod_e \mathrm{d}g_e\right) \chi_L\left(\prod_{e\in L} g_e\right) \mathrm{e}^{-S}, \tag{6.1}$$

where χ_L is the character of the irreducible representation carried by L. The expectation value corresponding to the Wilson loop is then $\mathcal{Z}[L]/\mathcal{Z}$. After expanding characters as in Section 4.1 we arrive at an expression

$$\mathcal{Z}[L] = \sum_{V_f} \left(\prod_f \alpha_{V_f}\right) \mathcal{Z}_{V_f}[L] \tag{6.2}$$

analogous to (4.4). The summand $\mathcal{Z}_{V_f}[L]$ takes the modified form

$$\mathcal{Z}_{V_f}[L] = \int \left(\prod_e \mathrm{d}g_e\right) \chi_L\left(\prod_{e\in L} g_e\right) \prod_f \chi_{V_f}\left(\prod_{e\in f} g_e\right). \tag{6.3}$$

We proceed as in Section 4.1 to obtain a diagrammatic representation. The characters are represented by diagrams (Fig. 4.1) and inserted into the lattice as wires. We only have an extra character χ_L now, which is inserted into the lattice as a wire along the edges designated by the data of the Wilson loop. Then the cables are inserted on the edges to represent the integrations. The only difference to Section 4.1 is that the cables for the edges of the Wilson loop now include the Wilson loop wire as well. We obtain a modified circuit diagram (see Fig. 6.1). The construction generalizes to several Wilson loops as well as to arbitrary spin networks inserted into the lattice along edges (with intertwiners positioned on vertices).

The generalization from conventional LGT to arbitrary symmetric categories is immediate by taking the modified circuit diagram as a definition. The generalization to nonsymmetric categories is less straightforward. The categorial structures needed to define the partition function in dimension n are related to isotopy in dimension $n-1$ since it is possible to confine the wires to the boundaries of the n-cells. However, as there is in general no canonical way of putting a Wilson loop on the boundaries of the n-cells, the categorial structures needed in the presence of a Wilson loop are those related to isotopy in dimension n. Indeed, we

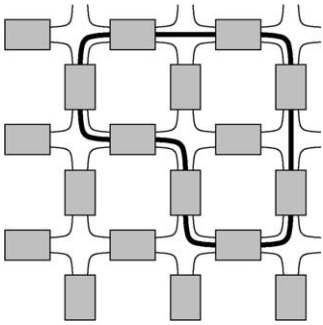

Fig. 6.1. A circuit diagram with a Wilson loop (thick line).

can define the value of a circuit diagram with Wilson loop in dimension 3 only for ribbon categories, and with the Wilson loop being framed. In dimension 4 there seems to be no obvious definition beyond the symmetric case.

In dimension 2 we can continue to use pivotal categories and the definition of the partition function extends to include Wilson loop and spin network observables in the obvious way.

To define the value of the circuit diagram with Wilson loop in dimension 3, we modify the construction of Section 4.2.1 as follows. As there we put the wire pieces onto the boundaries of the 3-cells. In contrast, we leave the ribbon that defines the Wilson loop completely inside the 3-cells, except of course were it pierces a 2-disk that defines a cable. These intersections of the ribbon with the 2-disks we choose such that they lie on the boundary of the 2-disks and the ribbon is aligned with the boundary, facing the outside direction. While in Section 4.2.1 we project just the boundary 2-spheres of the 3-cells onto the plane, now we project the whole 3-cells. However, we do this in such a way that the restriction of the projection to the boundary 2-spheres is precisely a projection of the boundary 2-sphere as in Section 4.2.1. Note that this involves making the same choices as there: a point in each 2-sphere and a point in each circle bounding a 2-disk (cable). Thus, after including the T-coupons, we arrive at a diagram that is exactly the same as the projected circuit diagram obtained in Section 4.2.1, except that we have extra ribbon pieces in it. Furthermore, these ribbon pieces can have crossings with the wire pieces. To obtain a proper ribbon diagram we only have to introduce the blackboard framing for the wire pieces. The value of the diagram defines the partition function with Wilson loop. Note that we can think of the framings of the wires as arising directly from the cellular decomposition. Indeed, frame the wires of the circuit diagram in the plane of the boundary 2-cells, face facing outwards from the 3-cell to which they belong. In that case we are even free to project the 3-cells without the projections restricting to projections of 2-spheres on the boundaries.

The proof of the independence of the value of the diagram from the choices made in obtaining it is almost the same as for the spherical case without Wilson loops. The main difference is that we now use the three-dimensional isotopy properties of ribbon graphs instead of the two-dimensional isotopy properties in the spherical case. Furthermore, there is one extra choice we have made, namely where to insert the Wilson loop ribbon into the boundaries of the 2-disks defining the cables. However, it is easy to see that a different

Table 2
Admissible types of categories for generalized LGT in different dimensions

Dim.	LGT	LGT + observable
≥5	Symmetric	Symmetric
4	Ribbon	Symmetric
3	Spherical	Ribbon
2	Pivotal	Pivotal

choice for a given cable just leads to extra braidings on both sides of the corresponding T-coupon in the final diagram, which are inverse (being mirror images). As the braiding is a morphism, it commutes with the T-projector (by property (d) in Fig. 2.6) and can thus be "pulled through" the T-coupon and "annihilated" with its inverse braiding. (Compare the proof for the four-dimensional ribbon case, Section 4.2.2.)

This construction generalizes in the obvious way to ribbon spin networks by including coupons. Thus, the observables in the three-dimensional ribbon case are framed Wilson loops or, more generally, ribbon spin networks embedded into the manifold.

The types of admissible category for LGT with and without observables are summarized in Table 2.

7. Boundaries and TQFT

Here we consider how our diagrammatic definition of the partition function extends to manifolds with boundary.

Let M be a cellular manifold of dimension n (oriented if the category is nonsymmetric) with boundary ∂M. (That is, a manifold with boundary having a cellular decomposition of the boundary that extends to a cellular decomposition of the manifold.) We can straightforwardly perform the construction of the circuit diagram in M, the only difference to the case without boundary being that we now have wire pieces with free ends on the boundary. These wire ends are actually inside cables that end on the boundary (see Figs. 7.1 and 7.2 for illustration). After projection, done in the usual way we now obtain a morphism not from the unit object **1** to itself, but between the unit object and the object associated with the boundary. We have the choice whether we want to consider this boundary object to determine the domain or image of the morphism. Diagrammatically, this is just the choice of writing the diagram such that all "loose" cable ends are aligned on the top (domain) or on the bottom (image). Note that changing this choice exchanges objects and dual objects as the arrows on the wires change their direction with respect to the vertical.

Assume for the moment that we have chosen the boundary object to lie in the image of the morphism. What is this boundary object? We have one cable for each vertex v of (the lattice associated with) the boundary (or $(n-1)$-cell). Each cable has a bunch of wires, with each piece of wire corresponding to one edge e meeting in v ($(n-2)$-cell bounding the $(n-1)$-cell "before identification"). Thus we have a tensor product $\otimes_{v\in\partial e} V_e$ as the object defined by the wires in that cable. The object corresponding to the whole boundary ∂M is the tensor product of all these objects. Thus, the (open) circuit diagram gives rise to

a morphism from **1** to this tensor product. However, we have not used the fact that there are cables around the wires on the boundary. Due to the decomposition property of the cables (Proposition 2.12), the total morphism decomposes into a tensor product of morphisms:

$$I_v : \mathbf{1} \to \bigotimes_{v \in \partial e} V_e \tag{7.1}$$

for each cable (and dual vertex v). (Note that this defines the individual morphisms I_v only up to scale. On the other hand the order of the I_v in the tensor product does not matter due to the identity $\mathbf{1} \otimes V = V \otimes \mathbf{1}$ for the category.) If we had made the other choice, namely that the boundary object should lie in the domain of the morphism we would have obtained a tensor product of morphisms of the type

$$I'_v : \bigotimes_{v \in \partial e} V_e \to \mathbf{1}. \tag{7.2}$$

We can also think of the morphisms (7.1) or (7.2) as states on the boundary, as they form vector spaces and can be paired in the obvious way. More precisely, a state would also

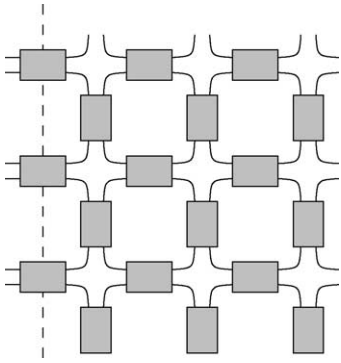

Fig. 7.1. The circuit diagram for a cellular manifold with boundary. The boundary is indicated by the dashed line.

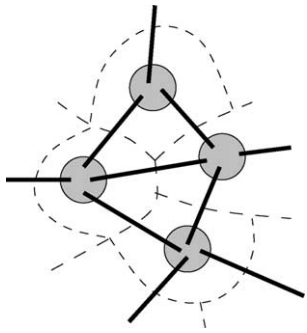

Fig. 7.2. The circuit diagram on the boundary. The $(n-1)$-cells are indicated by dashed lines. They are pierced by cables (represented as gray disks). The wires in the cables lie at the endpoints of the thick lines. These lines connect corresponding wire pieces. They are the edges of the spin network on the boundary.

include the specification of the labelings of the edges. Thus, the complete description of a state would be a labeling of the edges with arrows and simple objects, and a labeling of the vertices by morphisms (as specified by (7.1) or (7.2)) between the objects that label the incident edges. In fact, this is just an embedded spin network. We recover the well known picture of spin networks as states on the boundary of spin foams (see [7]). Note that to conform to our definition in Section 2.2 in the four-dimensional ribbon case we would expect the spin network to be a ribbon graph. We can indeed think of it in this way. To this end consider the circuit diagram embedded into the three-dimensional subcomplex as described in Section 4.2. The ribbons of the spin network are then obtained from the wire pieces that touch the boundary by removing their parts inside the manifold and gluing them together at the 2-cells on the boundary.

The states form a vector space since the morphisms form vector spaces and we can take the direct sum over the labelings of edges by objects. Thus, for a cellular manifold N of dimension $n-1$ we define the state space to be

$$\mathcal{H}_N := \bigoplus_{V_e} \left(\bigotimes_v \mathrm{Mor}\left(\bigotimes_{v\in\partial e} V_e, \mathbf{1} \right) \right). \tag{7.3}$$

The dual state space $\mathcal{H}_N^*$ is defined in the obvious way, by exchanging the arguments in Mor. (Note that this also exchanges objects with dual objects as diagrams are turned upside down.) The pairing between a state and a dual state is the obvious one if the labelings of edges coincide. Otherwise the pairing is defined to be zero.

Summing over all labelings, a cellular manifold M with boundary ∂M gives rise to a state (or dual state) and thus to a linear map $\mathbb{C} \to \mathcal{H}_{\partial M}$. (Note that in the case of infinitely many inequivalent simple objects we need to consider a completion of the direct sum in (7.3) to make this map algebraically well defined.) We use the usual weights α_V inside the manifold while we use a square root $\sqrt{\alpha_V}$ on the boundary, i.e., for the faces piercing the boundary. Dually, we can also think of this as giving rise to a linear form $\mathcal{H}_{\partial M} \to \mathbb{C} \cong \mathrm{Mor}(\mathbf{1}, \mathbf{1})$, by composition (pairing) with a spin network state. If ∂M consists of several connected components we can make different choices for the different components as to correspond to domain or image of such linear maps. In particular, let us assume that ∂M consists of two components $\partial M = \partial M_1 \cup \partial M_2$. Now defining ∂M_1 to correspond to the domain and ∂M_2 to the image we obtain a linear map

$$\Omega_{\partial M} : \mathcal{H}_{\partial M_1} \to \mathcal{H}_{\partial M_2} \tag{7.4}$$

in the obvious way.

Now assume we have two cellular manifolds M, M' with boundaries $\partial M = \partial M_1 \cup \partial M_2$ and $\partial M' = \partial M'_1 \cup \partial M'_2$, respectively, as well as a cellular homeomorphism identifying $\partial M_2 \cong \partial M'_1$. Gluing the manifolds together along ∂M_2, $\partial M'_1$ we obtain a new one $M'' = M \cup M'$ with boundary $\partial M'' = \partial M_1 \cup \partial M'_2$. This gives rise to linear maps Ω_M, $\Omega_{M'}$ and $\Omega_{M''}$ satisfying the composition property

$$\Omega_{M''} = \Omega_{M'} \circ \Omega_M. \tag{7.5}$$

This is because the circuit diagram for M'' is just the same as the ones for M' and M attached to each other. This is also true for the projections (in the symmetric as well as the nonsymmetric cases) which define its values, as the attachment is only between cables/T-coupons.

Note that we use the projector property (c) of the T-coupon (Fig. 2.6) as in attaching the circuit diagrams we have cables on both sides which we then "glue" to single cables. Furthermore, the weights $\sqrt{\alpha_V}$ on the boundary recombine to the usual weights α_V.

The state space of spin networks is complete in the following sense. Take the situation above with the manifolds M, M', etc. The spaces $\mathcal{H}_{\partial M_2}$ and $\mathcal{H}_{\partial M_1'}$ are identified. Taking a basis $|\psi\rangle$ of $\mathcal{H}_{\partial M_1'}$ (consisting of a basis of morphisms for each labeling of edges) and the dual basis $\langle\psi|$ of $\mathcal{H}^*_{\partial M_2}$ we can write this as

$$\sum_{\psi} \Omega_{M'}|\psi\rangle\langle\psi|\Omega_M = \Omega_{M'} \circ \Omega_M. \tag{7.6}$$

Diagrammatically, this is just the insertion of decompositions for the cables crossing the common boundary, as well as writing the sum over labelings of the wires crossing the boundary explicitly.

What we arrive at is "almost" a TQFT. The topological objects are cellular manifolds of dimension $n-1$ and their cellular cobordisms. This forms "almost" a category. (The notion of identity morphism is lacking.) On the other hand we have the category of vector spaces and linear maps. What we obtain is thus "almost" a functor from the "cellular cobordism category" to the category of vector spaces by assigning state spaces to cellular manifolds and linear maps to cellular cobordisms. In particular, the crucial composition property (7.5) is satisfied. In the topologically invariant case (i.e., when the partition function is independent of the cellular decomposition, see Section 8.2) one can forget about the cellular decomposition of the cobordism. The identity in the cobordism category is then the "cylindrical" cobordism; for a manifold N, this is $I \times N$ with I a closed interval. Quotienting the state space $\mathcal{H}_N$ by the kernel of $\Omega_{I\times N}$ then gives rise to a TQFT. See [14] for this kind of quotient construction.

It is straightforward to combine boundaries and Wilson loop (or spin network) observables. Now the manifolds are allowed to have Wilson loops embedded in them, which may end on the boundary. Thus, the boundaries are cellular manifolds with possible extra labels on their vertices indicating the object label of a Wilson loop L piercing the boundary at this vertex. The morphisms (and states) on the boundary are modified so as to include the extra objects. The change is just the inclusion of the the object as an extra factor V_L in the tensor product $(\otimes_{v\in\partial e} V_e) \otimes V_L$ for this vertex. Everything else in the above construction works as before. Thus, we obtain "almost" a TQFT. Now it is defined on the "almost category" of cellular manifolds with possible extra object labels on the dual vertices. The cobordisms are now cellular manifolds which have Wilson loops (or more generally spin networks) embedded, as discussed in Section 6, with corresponding labels. This works now for symmetric categories in any dimensions, and for ribbon categories in dimension 3. In fact, in the latter case, as the Wilson loops are ribbons, there is slightly more structure not only on the cobordisms (as already discussed in Section 6), but also on the boundaries. The ends of the Wilson loops on the boundary need to be considered as carrying a direction which determines the framing. This is similar to a situation considered in [23], where a TQFT with Wilson loops in dimension 3 is constructed from the surgery invariants of [13].

Finally (without working out any details) we mention that given extra complex structure on the category, we can make the state spaces into Hilbert spaces. For example, if the

category is the category of representations of a compact Lie group we can identify dual representations as conjugate representations. Thus, we obtain Hilbert space structures on the representations and in turn on the relevant intertwiner spaces (between the trivial and an arbitrary representation).

8. Special cases

8.1. Spin foams and nj-symbols

We discuss here how the conventional picture of spin foam models employing polyhedral "recoupling diagrams" is recovered. Consider a cable around a number of wires carrying object labels $V_1, \ldots, V_n$ representing the morphism $T_{V_1 \otimes \cdots \otimes V_n}$. By definition (Proposition 2.12), we can decompose it into morphisms $\Phi_i : V_1 \otimes \cdots \otimes V_n \to \mathbf{1}$ and $\Phi_i' : \mathbf{1} \to V_1 \otimes \cdots \otimes V_n$ such that

$$T_{V_1 \otimes \cdots \otimes V_n} = \sum_k \Phi_k' \Phi_k. \tag{8.1}$$

We depict this diagrammatically as in Fig. 8.1. The morphisms are here represented by coupons which are shrunk to dots. Note that the dashed line representing the unit object **1** is normally omitted and here only drawn for illustration.

We can introduce such a decomposition for every cable in a circuit diagram. The resulting graph then consists of disconnected polyhedral diagrams, one for each n-cell (or vertex of the associated lattice). The lines of the polyhedra are the wires while its corners arise where the wires entered a cable. The partition function now has an extra summation besides the one over labelings of faces with simple objects. This is the summation over the decomposition (8.1) for every edge. Thus, we can express the partition function as

$$\mathcal{Z} = \sum_{V_f} \left(\prod_f \alpha_{V_f} \right) \sum_{\Phi_e} \prod_v A_v(V_f, \Phi_e). \tag{8.2}$$

Here, Φ_e denotes a morphism between the tensor product of objects corresponding to the wires on the edge e, and we sum over labelings with such morphisms as prescribed by (8.1). A_v denotes the value of the polyhedral diagram arising at the vertex v. It depends on the labelings of the faces and edges that meet in v.

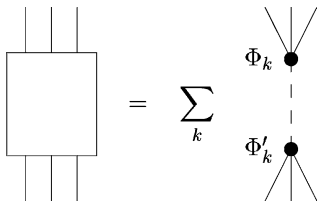

Fig. 8.1. Decomposition of the T-morphism on a tensor product.

Formula (8.2) is essentially the general definition of a spin foam model, except that one usually requires the weight α_V to be the dimension of the representation V, i.e., $\alpha_V := \dim_V$ (or for general categories $\alpha_V := \mathrm{loop}_V$). For general spin foam models, one has some freedom in defining the "vertex amplitude" A_v. The one we obtain here (defined by the polyhedral diagrams as described above and with the special choice of weights) defines the spin foam models of BF-type. These are topological and give rise to state sum invariants (see the next section).

Usually one chooses bases of the decompositions (8.1) in a globally coherent way for the whole category so that they can be indexed. However, there is no canonical way of doing this. One can compare this to a choice of "coordinates". In this sense, the circuit diagram formulation of the partition function is "coordinate-free". In contrast, for a definition that starts out from (8.2), one would have to show independence of $\mathcal{Z}$ under the choice of bases.

The spin foam approach (and related state sum models) are normally restricted to a simplicial decomposition of the manifold. This has the effect that the number of edges meeting in a vertex and the number of faces bounded by an edge is a fixed number just depending on the dimension of the manifold. This means that just one type of polyhedral diagram with fixed number of edges and vertices appears. Thus, one has only one type of "recoupling symbol" as such polyhedral diagrams are called. For example, in dimension 3 this is a $6j$-symbol and in dimension 4 a $15j$-symbol. The standard approach at showing that a state sum of the type (8.2) is well defined (or even a topological invariant) is by using properties of these recoupling symbols. Of course, this seems rather hopeless if infinitely many types of recoupling symbols can occur, hence the restriction to simplicial decompositions.

8.2. Weak coupling limit, state sum invariants and BF-theory

For conventional LGT (with a compact Lie group G) one requires the local action σ (4.1) to recover the continuum action of Yang–Mills theory in the limit of small lattice spacing. In particular, σ will be a function of the coupling constant λ of the continuum theory. Then, the Boltzmann weight $\mathrm{e}^{-\sigma(\lambda,g)}$ tends to the delta function $\delta(g)$ in the weak coupling limit $\lambda \to 0$. Thinking of the partition function as a path integral over connections, this means that only flat connections contribute. In terms of the weights, this limiting case is $\alpha_V = \dim V$. In our formulation, there is nothing manifestly singular about this case. However, the partition function $\mathcal{Z}$ will in general not converge anymore. An alternative way to obtain this partition function is as a discretization of BF-theory. Integrating out the B-field yields the delta function on the connection.

The attractive feature about BF-theory is that it is a topological theory. That means, the discretized partition function depends only on the topology of the manifold. It is the same (up to a factor) for any cellular decomposition of it. This extends beyond the group case and for the various categories we have considered the "topological" weight is given by $\alpha_V = \mathrm{loop}\, V$. Indeed, our construction recovers the various state sum invariants in this case. While for group representations $\mathrm{loop}\, V = \dim V$, we have $\mathrm{loop}\, V = \mathrm{sdim}\, V$ (the super-dimension) in the supergroup case and $\mathrm{loop}\, V = \mathrm{qdim}\, V$ (the quantum dimension) in the quantum group case.

In two dimensions the situation is rather simple (as LGT is then solvable). Consider a compact connected oriented 2-manifold M with some cellular decomposition and a pivotal category $\mathcal{C}$. Induce the orientations of the faces of the associated lattice from M. Project onto the plane with positive (anti-clockwise) orientation and set $\alpha_V := \mathrm{loop}_- V$. We apply the identity of Proposition 2.14 to all cables of the circuit diagram. If any two adjacent faces are labeled with different objects, the partition function vanishes. Thus, we have only one sum over simple objects. All the cables are replaced with the diagram at the right hand side of Fig. 2.9. Thus, we just obtain a bunch of loop diagrams with negative (clockwise) oriented arrows. Indeed, we obtain one loop for each vertex (2-cell), one inverse loop for each edge (1-cell) and one loop for each face (0-cell), from the weight. Consequently

$$\mathcal{Z} = \sum_V (\mathrm{loop}_- V)^\chi \tag{8.3}$$

with $\chi = n_2 - n_1 + n_0$ the Euler characteristic of M (n_i the number of i-cells). (Note that we could have equally chosen $\alpha_V := \mathrm{loop}_+ V$ and projected with negative orientation. This has the same effect as interchanging V and V^*. Thus, the resulting $\mathcal{Z}$ is the same.)

In higher dimensions the above-mentioned factor has to be taken into account to obtain a true invariant. The invariant is

$$\tilde{\mathcal{Z}} := \kappa^{-\chi_L}\mathcal{Z} \quad \text{with} \quad \kappa := \sum_V (\mathrm{loop}\, V)^2 \tag{8.4}$$

and χ_L is the "Euler characteristic" of the associated lattice. That is $\chi_L := n_v - n_e + n_f = n_d - n_{d-1} + n_{d-2}$ in dimension d. As $\chi_L = \chi$ an invariant in two dimensions there was no need for this factor in that case.

In three dimensions for SU(2) we recover the Ponzano–Regge model [9], which yields a divergent partition function as the sum over representation labels is infinite. For $\mathrm{SU}_q(2)$ at a root of unity (giving rise to a ribbon category, see next section) we recover the Turaev–Viro state sum [14], which defines interesting 3-manifold invariants. The generalization to spherical categories (to which our definition extends) was achieved by Barrett and Westbury [20]. The proof of topological invariance in our framework turns out to be surprisingly simple, as it can be cast purely in the diagrammatic language [30]. In fact, while previous proofs have employed simplicial decompositions, the generalization to cellular decompositions makes the proof even simpler. This is because it can be cast in terms of moves between cellular decompositions which correspond to "elementary" diagrammatic identities.

In four dimensions, the group SU(2) yields Ooguri's analogue [31] of the Ponzano–Regge model. The quantum group $\mathrm{SU}_q(2)$ yields the invariant of 4-manifolds of Crane and Yetter [16], later generalized to ribbon categories [17]. The proof of topological invariance in our framework should be very similar to the three-dimensional one.

8.3. Modular categories and chain mail

Interesting (finite and nontrivial) examples of state sum invariants on the one hand and models of quantum gravity with cosmological constant [10] on the other hand are obtained from q-deformed groups at roots of unity. These give rise to quasimodular categories (in the

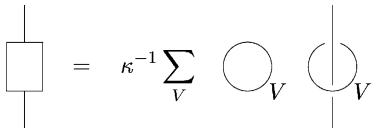

Fig. 8.2. Identity for the T-morphism in a modular category. The sum runs over equivalence classes V of simple objects. The arrow directions on the loops are irrelevant and blackboard framing is implied.

terminology of Turaev [23]) with finitely many equivalence classes of simple objects. Although these categories are not semisimple, they can be turned into semisimple ones through a process of "purification". This is a quotient construction on the morphism spaces [23]. The obtained categories are *modular*, a special case of ribbon categories with a nondegeneracy condition on the braiding.

For modular categories the T-morphism can be expressed as a sum over diagrams with a loop going round a line (see Fig. 8.2). (κ is defined as above.) Consider the three-dimensional setting specialized to modular categories. The circuit diagram can be constructed as a ribbon diagram freely embedded into the cellular manifold (not restricted to the two-dimensional subcomplex) (see Section 6). As the cables of the embedded circuit diagram are disks (shortened cylinders), we can use the above identity to replace them by loops going round the wire strands. This converts the circuit diagram into a pure ribbon link. We obtain one extra summation over simple objects for each replaced cable. $\mathcal{Z}_{V_f}$ of Definition 4.2 is thus decomposed as

$$\mathcal{Z}_{V_f} = \kappa^{-n_e} \sum_{V_e} \mathcal{Z}_{V_f, V_e} \tag{8.5}$$

with n_e the number of edges and the sum ranging over all labelings V_e of edges with equivalence classes of simple objects. The value $\mathcal{Z}_{V_f, V_e}$ is now given by the Reshetikhin–Turaev invariant [13] (in its TQFT normalization) of the labeled ribbon link in the given manifold. This is (in the topological case) essentially a categorial analogue of Robert's Skein theoretic "chain mail" construction of the Turaev–Viro invariant [32].

8.4. Comparison with previous generalizations of LGT

In the three-dimensional case Boulatov [5] put forward a proposal for q-deformed LGT. Indeed, this proposal amounts essentially to the chain mail construction of modular LGT considered above.

In the four-dimensional case Pfeiffer [6] recently constructed a ribbon category generalization of LGT for simplicial decompositions of the underlying manifold. Our partition function specializes to his in the simplicial case. However, as general LGT is not topological, the generalization to cellular decompositions is a substantial improvement. For example, hypercubic lattices (commonly used in LGT) arise from cellular decomposition that are not simplicial.

9. Outlook

In this closing section we discuss several possible developments suggested by the present work.

For (ordinary) LGT, the diagrammatic formulation of the partition function introduced here is a further step in developing the dual model [3]. In the strong-coupling regime, contributions to the partition function with "small" representation labels dominate. The diagrammatic techniques introduced here should help to deal with those contributions in order to extract a strong-coupling expansion. On the other hand, the weak coupling regime is equally accessible through our formalism. Indeed, the proof of topological invariance in the limit employs elementary diagrammatic identities [30]. The "expansion" of these identities might thus lead to an "expansion" of LGT around this topological limit. This would provide a new type of weak coupling expansion (not destroying the global structure of the gauge group) possibly shedding new light on the continuum limit.

The generalization of LGT beyond groups might be useful in several ways. First of all, it makes it possible to put supersymmetric gauge theories on the lattice. It would be interesting to see how improvements of convergence and renormalizability of such theories manifest themselves on the lattice. Going further, LGT with quantum gauge groups could be something very natural. This is suggested by the (related) observations that "quantization" of the group can occur both in making sense of a divergent path integral [4] or in introducing a term in the Lagrangian which corresponds to a cosmological constant [10]. Indeed, the regularizing effect of q-deformed groups at roots of unity is immediately apparent in our LGT framework, as it makes the set of equivalence classes of simple objects finite and thus the partition function manifestly finite and well defined.

For BF-theory one immediate application of our formalism is three-dimensional quantum supergravity. Indeed, in the same way that BF-theory with gauge group SO(3) or SO(2,1) describes pure gravity in three dimensions, BF-theory with OSp supergroups describes supergravity in three dimensions [33]. Furthermore, in the same way as quantum BF-theory is also in higher dimensions a starting point for quantum gravity one could consider quantum BF-theory with the relevant supergroup a starting point for quantum supergravity. In particular, this might be of interest in string theory, where 11-dimensional supergravity is considered one limit of the conjectured M-theory. A promising model for pure quantum gravity in four dimensions was proposed by Barrett and Crane [11]. This is based on a modification of BF-theory in its spin foam formulation. Nevertheless, the Barrett–Crane model can still be expressed in the diagrammatic language introduced here. Thus, the diagrammatic methods here might help in understanding and developing this model and its "relatives".

An open problem in approaches to quantum gravity is how to perform a "sum over topologies". Recently, a proposal has been made to generate spin foams (i.e., essentially topologies) as Feynman graphs of a quantum field theory of fields living on the gauge group [34]. On the other hand it has been shown in [35] how Feynman diagrams can be rigorously considered as diagrams denoting morphisms (in the sense of Section 2.2) in the category of representations of the symmetry group of the quantum field theory. Thus, for such generating field theories we obtain immediately a representations of the emerging spin

foams (space–times) in terms of the diagrammatics introduced here (using, in particular Section 3.1). Furthermore, the main emphasis in [35] was the generalization to braided categories (similar to ribbon categories). Thus, this provides a way to extend such generating field theories to quantum groups in the necessary absence of additional topological input (as we required in Section 4.2).

Acknowledgements

I would like to thank H. Pfeiffer, A. Perez, F. Girelli and M. Reisenberger for valuable discussions and comments on the manuscript. This work was supported by a NATO fellowship grant.

References

[1] R. Savit, Duality in field theory and statistical systems, Rev. Mod. Phys. 52 (1980) 453–487.
[2] M.P. Reisenberger, Worldsheet formulations of gauge theories and gravity, 1994, Preprint gr-qc/9412035.
[3] R. Oeckl, H. Pfeiffer, The dual of pure non-Abelian lattice gauge theory as a spin foam model, Nucl. Phys. B 598 (2001) 400–426.
[4] E. Witten, Quantum field theory and the jones polynomial, Commun. Math. Phys. 121 (1989) 351–399.
[5] D.V. Boulatov, q-Deformed lattice gauge theory and 3-manifold invariants, Int. J. Mod. Phys. A 8 (1993) 3139–3162.
[6] H. Pfeiffer, Four-dimensional lattice gauge theory with ribbon categories and the Crane–Yetter state sum, J. Math. Phys. 42 (2001) 5272–5305.
[7] J.C. Baez, Spin foam models, Class. Quant. Grav. 15 (1998) 1827–1858.
[8] E. Witten, $(2+1)$-Dimensional gravity as an exactly soluble system, Nucl. Phys. B 311 (1988/1989) 46–78.
[9] G. Ponzano, T. Regge, Semiclassical limit of Racah coefficients, in: F. Bloch, et al. (Eds.), Spectroscopic and Group Theoretical Methods in Physics, North-Holland, Amsterdam, 1968.
[10] S. Major, L. Smolin, Quantum deformation of quantum gravity, Nucl. Phys. B 473 (1996) 267–290.
[11] J.W. Barrett, L. Crane, Relativistic spin networks and quantum gravity, J. Math. Phys. 39 (1998) 3296–3302.
[12] J.C. Baez, An Introduction to Spin Foam Models of BF Theory and Quantum Gravity, Geometry and Quantum Physics, Schladming, 1999, Lecture Notes in Physics, No. 543, Springer, Berlin, 2000, pp. 25–93.
[13] N.Yu. Reshetikhin, V.G. Turaev, Invariants of 3-manifolds via link polynomials and quantum groups, Invent. Math. 103 (1991) 547–597.
[14] V.G. Turaev, O.Ya. Viro, State sum invariants of 3-manifolds and quantum 6j-symbols, Topology 31 (1992) 865–902.
[15] J.W. Barrett, B.W. Westbury, Invariants of piecewise-linear 3-manifolds, Trans. Am. Math. Soc. 348 (1996) 3997–4022.
[16] L. Crane, D. Yetter, A Categorical Construction of 4D Topological Quantum Field Theory, Quantum Topology, Dayton, 1992, Series on Knots and Everything, Vol. 3, World Scientific, Singapore, 1993, pp. 120–130.
[17] L. Crane, L.H. Kauffman, D.N. Yetter, State-sum invariants of 4-manifolds, J. Knot Theory Ram. 6 (1997) 177–234.
[18] P.J. Freyd, D.N. Yetter, Braided compact closed categories with applications to low dimensional topology, Adv. Math. 77 (1989) 156–182.
[19] N.Yu. Reshetikhin, V.G. Turaev, Ribbon graphs and their invariants derived from quantum groups, Commun. Math. Phys. 127 (1990) 1–26.
[20] J.W. Barrett, B.W. Westbury, Spherical categories, Adv. Math. 143 (1999) 357–375.
[21] S. Mac Lane, Categories for the Working Mathematician, 2nd Edition, Springer, New York, 1998.
[22] R. Penrose, Angular momentum: an approach to combinatorial space–time, in: T. Bastin (Ed.), Quantum Theory and Beyond, Cambridge University Press, Cambridge, 1971, pp. 151–180.

[23] V.G. Turaev, Quantum Invariants of Knots and 3-Manifolds, de Gruyter, Berlin, 1994.
[24] R. Carter, G. Segal, I. MacDonald, Lectures on Lie Groups and Lie Algebras, Cambridge University Press, Cambridge, 1995.
[25] S. Majid, Foundations of Quantum Group Theory, Cambridge University Press, Cambridge, 1995.
[26] R. Oeckl, The Quantum Geometry of Supersymmetry and the Generalized Group Extension Problem, J. Geom. Phys. 44 (2002) 299–330.
[27] W.S. Massey, A Basic Course in Algebraic Topology, Springer, New York, 1991.
[28] M. Creutz, Quarks, Gluons and Lattices, Cambridge University Press, Cambridge, 1983.
[29] M. Creutz, Gauge fixing, the transfer matrix, and confinement on a lattice, Phys. Rev. D 15 (1977) 1128–1136.
[30] F. Girelli, R. Oeckl, A. Perez, Spin foam diagrammatics and topological invariance, Class. Quant. Grav. 19 (2002) 1093–1108.
[31] H. Ooguri, Topological lattice models in four dimensions, Mod. Phys. Lett. A 7 (1992) 2799–2810.
[32] J. Roberts, Skein theory and Turaev–Viro invariants, Topology 34 (1995) 771–787.
[33] A. Achúcarro, P.K. Townsend, A Chern–Simons action for three-dimensional anti-de Sitter supergravity theories, Phys. Lett. B 180 (1986) 89–92.
[34] M. Reisenberger, C. Rovelli, Space–time as a Feynman diagram: the connection formulation, Class. Quant. Grav. 18 (2001) 121–140.
[35] R. Oeckl, Braided quantum field theory, Commun. Math. Phys. 217 (2001) 451–473.